# Chapter 3
# Inorganic Photochemistry

**Julia A. Weinstein**

**Abstract** The fascinating field of inorganic photochemistry is extremely diverse. This chapter discusses some general principles governing light-induced properties of metal-containing molecular compounds. The great variety of excited states of different nature—far greater than those available in organic compounds—accessible in metal-containing species is discussed, and linked to various photochemical transformations. The emphasis is placed on the diversity and open-end possibilities to use wavelength-dependent reactivity of such species for creating a variety of products. Modern methods for the interrogation of excited states on ever faster time scales are briefly outlined. Recent technological advances open up exciting prospects of modulating the outcome of photochemical reactions by altering the earliest photo-events. It is clear that inorganic photochemistry will continue to play a central role in light-driven applications.

## 3.1 Introduction

The general principles of the interaction of light with metal-containing compounds described in this chapter follow the same general rules as those already introduced in Chap. 1.

There are several important features which distinguish photophysical and photochemical properties of metal-containing compounds from those of organic molecules.

J. A. Weinstein (✉)
Department of Chemistry, University of Sheffield, Sheffield S3 7HF, UK
e-mail: Julia.Weinstein@sheffield.ac.uk

R. C. Evans et al. (eds.), *Applied Photochemistry*,
DOI: 10.1007/978-90-481-3830-2_3,

1. Metal-containing species offer a much greater diversity of types of excited state compared to organic molecules because of the participation of metal orbitals in addition to ligand orbitals.
2. A manifold of several excited states of different origin close in energy to one another is an intrinsic feature of metal-containing species. Due to their different origin and often different spatial localization, internal conversion between these states is not always efficient. This intriguing property results in several excited states being independently emissive and/or reactive, thus violating one of the main rules developed for organic photochemistry, *viz.* Kasha's rule [1] (Chap. 1). This feature gives rise to exciting phenomena such as multiple emission, or excited state branching, where the nature of the products and their yields depend on the excitation wavelength, such that a control of photochemical pathways is in principle possible.
3. The energy of the lowest optically accessible excited state frequently lies in the visible spectral range, enabling photochemical transformations to be accomplished with visible light.
4. The presence of the heavy metal atom induces strong spin–orbit coupling, considerably relaxing the spin selection rule and resulting in fast or ultrafast intersystem crossing. Thus long-lived, low-energy triplet excited states are readily accessible, enabling many applications.
5. The almost modular structure of transition metal complexes—$Ligand_1$-Metal-$Ligand_2$—brings about synthetic versatility inaccessible with organic compounds. It is possible to adjust the periphery of a complex to meet a particular requirement—tuning the energy of the lowest electronic transition, controlling solubility, adding functional groups required for attachment to surfaces, etc.—whilst maintaining both the immediate coordination sphere of a metal complex and the nature of the lowest excited state.

The photophysics, photochemistry and applications of transition metal complexes are the subjects of several comprehensive books [2–5] and recent reviews [6–9]. Hence, we will only briefly present the basic aspects of this broad field. We

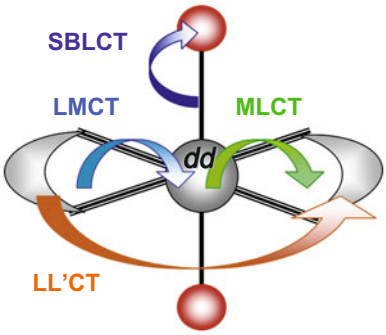


**Fig. 3.1** Main types of excited state in transition metal complexes

start from the description and classification of different types of electronic excited state which can be potentially formed in metal-containing species (Fig. 3.1), and follow with some examples of reactions for each type of the excited state.

## 3.2 The Two Timescales

The photochemistry and photophysics of metal-containing compounds can occur in two very different time domains: 'ultrafast' (from a non-equilibrated excited state), and 'slow', from thermally-equilibrated excited states. The distinction is not often clear, but it is important to note that a thermally equilibrated excited state has reached Boltzmann distribution, and is usually considered to be in the lowest vibrational level on the corresponding potential energy surface. Such excited states can possess a very long lifetime, from nanoseconds to milliseconds or even longer. They can be regarded as independent species—a higher energy 'isomer' of the ground state—whose reactivity can be described by equilibrium thermodynamics and transition state theory.

In contrast, 'ultrafast' photochemistry frequently occurs from a non-equilibrated, higher lying and/or vibrationally 'hot' excited states, in which the reaction takes place from a vibrational level higher than the zero level of the relevant electronic excited state. This phenomenon is partly due to the fact that Frank–Condon (FC) electronic excited states are usually formed vibrationally 'hot', due to the relative displacement of the potential energy surface of the excited state with respect to that of the ground state. Energy dissipation from the FC state leading to the population of the zero vibrational level of the final electronic state involves three main processes: vibrational relaxation, intramolecular vibrational energy redistribution, and transfer of energy to the solvent. The overall process usually takes from several picoseconds if organic groups are involved, to several tens of picoseconds if the coupling between the group in question and the rest of the molecule is weak, as is often the case with, for example, metal carbonyls. An example of an ultrafast process originating from a non-relaxed excited state is intersystem crossing in metal complexes, in which the heavy atom effect facilitates spin–orbit coupling, leading to the rates of intersystem crossing (ISC) being on the scale of tens/hundreds of femtoseconds—orders of magnitude faster than in organic molecules. More generally, examples include 'predissociation' [1] or any ultrafast photodissociation, which occur on a timescale faster than relaxation to the zero vibrational level of the lowest excited state. Of course processes occurring on different photochemical time scales are closely interrelated—the formation and reactions of vibrationally relaxed electronically excited states follows from the ultrafast steps. A special type of non-equilibrated excited state process is when a chemical reaction occurs from a non-zero vibrational level of the *ground* electronic state—this type of reactivity is sometimes termed *infrared photochemistry*.

The distinction between 'non-relaxed' and 'relaxed, equilibrium' photochemistry has been acknowledged for a long time [10]. However, only recently with the

advent of ultrafast methods has it become possible to directly follow the processes involving vibrationally 'hot' excited states in real time [11]. Here, we define the *ultrafast* scale in condensed media as that from femtoseconds to the completion of vibrational relaxation, *i.e.* tens to hundreds of picoseconds. From the point of view of experimental observations, vibrational relaxation is accompanied by a shift of the absorption bands in the electronic transient absorption (TA) spectrum. The process is considerably more evident in the transient infrared spectra, where vibrational cooling from e.g. $v' = 1$ to $v' = 0$ is accompanied by a disappearance of the absorption due to $v'_1 \rightarrow v'_2$ (or transitions involving higher vibrational levels) and an increase in the intensity of the absorption band due to $v'_0 \rightarrow v'_1$. A narrowing of the transient IR bands is also observed in the course of vibrational relaxation. An emerging method for study of vibrational relaxation is transient two-dimensional infrared spectroscopy (T-2DIR) which allows direct insight into the dynamics of vibrational energy redistribution in the interrogated system [12, 13]. T-2DIR also has the power to resolve coupling between individual vibrational modes in the excited state(s), as well as coupling between intermolecular and solvent vibrational modes accompanying a particular excited state reaction, thus providing a new insight into reaction mechanisms in photochemistry.

In order to obtain a complete picture of the excited states of a metal complex, a combination of time-resolved spectroscopic techniques are typically used. Transient electronic spectroscopy is the most common tool to follow dynamics of the excited states. In this type of transient spectroscopy, the probe pulse usually is in the UV/Vis part of the spectrum. However, the electronic absorption spectra of excited states are generally very broad and not always distinct. Therefore, if multiple excited states are formed, electronic spectroscopy is best combined with time-resolved vibrational spectroscopy. Time-resolved vibrational spectroscopy (TRVS) provides a powerful and complementary method to resolve a manifold of close-lying excited states because it probes molecular structure. TRVS is also invaluable for elucidating the dynamics of vibrationally hot electronic states which are frequently formed upon initial photo-excitation and play a key role in the ultrafast intramolecular energy redistribution. The frequently used types of TRVS are time-resolved infrared (TRIR) [9], and time-resolved Raman methods. TRIR uses UV/Vis excitation and probe/detection in the mid-IR range of the spectrum, typically from 1200 up to 2500 $cm^{-1}$. It was initially applicable mainly to molecules bearing strong IR-reporters such as C=O, or C≡C, or C≡N [14]. Major developments in detector sensitivity have made it possible to investigate much weaker IR bands, essentially covering the entire molecular framework. Changes in the *energy* of the infrared bands of a metal complex in the excited state, if compared to the ground state, indicate changes of electron density distribution, and assists in assignment of the nature of the excited states involved. Changes in the relative *intensity* of the IR bands between ground and excited electronic states can yield further structural information.

The combined use of spectroelectrochemical and time-resolved IR methods, which illustrates the value of complementary methods used in parallel, is illustrated in Fig. 3.2, for a Pt(II) diimine complex $Pt(bpyam)Cl_2$, bpyam = 4,4′-$\{C(O)NEt_2\}_2$-2,2′-bipyridine [15]. The bottom panel in Fig. 3.2 demonstrates the

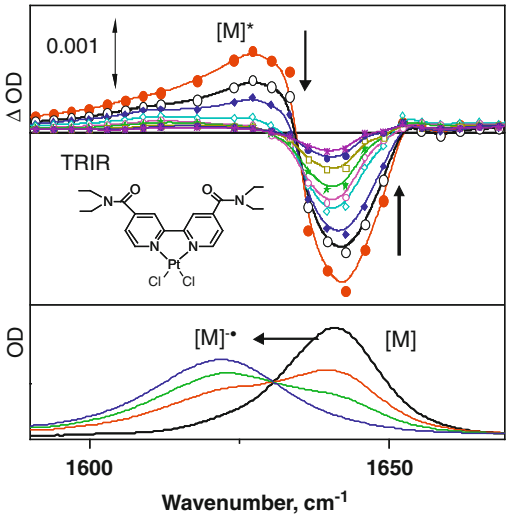


**Fig. 3.2** *Bottom panel*: ground state FTIR spectrum (*black*) and a series of spectra obtained in the course of electrochemical reduction. *Top panel*: a series of TRIR spectra of $Pt(bpyam)Cl_2$ in $CH_2Cl_2$, recorded at 1, 2, 3, 5, 7, 10, 15, 20 and 25 ps time delays after initial excitation with a 400 nm, ~150 fs laser pulse [15]

19 $cm^{-1}$ shift to lower energy of the $\nu$(CO) of the neutral molecule upon electrochemical reduction to $[Pt(bpyam)Cl_2]^{-\bullet}$. This species, according to density functional theory (DFT) calculations, should be represented as $[Pt(bpyam^{-\bullet})Cl_2]$ following a ligand-centred reduction, with an excess of electron density on the $\pi^*$ orbital which is largely –C=O localised. On the other hand, upon promotion to the excited state, the ground-state $\nu$(CO) is transiently shifted to lower energy by about the same amount such that it almost coincides with $\nu$(CO) of $[Pt(bpyam)Cl_2]^{-\bullet}$. Thus, the TRIR behaviour is consistent with the Pt → bpyam metal-to-ligand charge transfer (MLCT) nature of the lowest excited state, in which the same $\nu$(CO) $\pi^*$ antibonding orbital is populated.

Another type of TRVS, time-resolved resonance Raman spectroscopy, highlights vibrations coupled to a particular electronic transition in the excited state, assisting in assignment of the nature of the frontier orbitals [16, 17].

Apart from optical methods aleady mentioned above a plethora of other methods for characteristing excited states exist, including application of X-rays for direct structural interrogation of transient species. Time-resolved X-ray diffraction and X-ray absorption spectroscopy [X-ray absorption near edge structure (XANES), and the extended X-ray absorption fine structure (EXAFS)] allow unprecedented insight into both dynamics and structure of short-lived excited states [18–22]. Another interesting aspect of modern inorganic photochemistry is the use of various reaction media such as low-temperature matrices to trap reactive intermediates, supercritical fluids [23] or ionic liquids [24] to encourage reaction conditions not accessible in conventional solvents.

Inorganic photochemistry embraces all modern methods, rapidly developing with the increasing technological advances in excitation sources and detectors, which make accessible detection and measurement of ever faster processes, and ever more elusive reaction intermediates and excited states.

## 3.3 Classification of Excited States in Transition Metal Complexes

The photoreactivity of an excited state depends largely on its energy, lifetime, and the nature of the orbitals involved. It is therefore important to provide classification of the most common types of excited state in metal-containing species.

### *3.3.1 Intra-Ligand Excited States (IL)*

Most intra-ligand (also called ligand-centred) transitions will remain upon coordination of the ligand to the metal centre, although their energies may be somewhat perturbed, and the rates of intersystem crossing (hence emission lifetimes and yields) may be strongly affected by the metal centre due to the heavy atom effect. Examples of IL transitions include $\pi \rightarrow \pi^*$ or $n \rightarrow \pi^*$ transitions. Examples of coordination compounds whose lowest excited states are ligand-centred include metalloporphyrins as well as some metal complexes such as $[Rh(bpy)_3]^{3+}$ or $[Zn(terpy)_2]^{2+}$ in which the metal centre is redox inactive.

Given the focus of this chapter on metal complexes, we concentrate below on those types of electronic transitions which either involve directly, or are affected by, the metal centre. These involve metal-centred transitions such as *dd* or *ff*; charge-transfer metal/ligand transitions (metal-to-ligand or ligand-to-metal), and transitions between different ligands which can only occur because they are anchored to the same metal ion.

### *3.3.2 Metal-Centred Excited States: dd*

According to ligand field (LF) theory, the energy of the MC (LF) state depends on the ligand and on the metal centre (Fig. 3.3) [25].

For a given ligand, the ligand field splitting increases with the increase of the number of electrons of the central atom, thus following the trend 1st row transition metals $<$ 2nd row transition metals $<$ 3rd row transition metals, and therefore the energy of the LF transitions follow the same trend. The important consequences for photophysics and photoreactivity are that LF states are much more often lowest

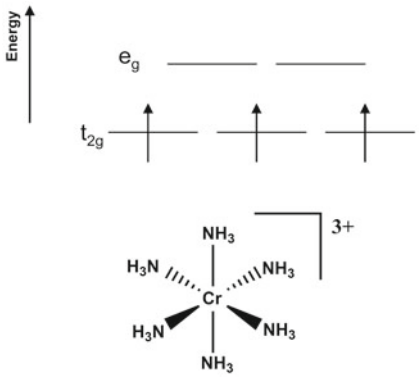


**Fig. 3.3** An example of a Cr(III) complex

in energy in complexes of 1st and 2nd transition metal complexes, and frequently determine their photoreactivity. A typical example, which we will discuss in detail below, is ligand dissociation, initiated by a ligand field transition corresponding to electron density shift from a metal-ligand non-bonding to a metal-ligand anti-bonding orbital. A classical example is photosubstitution of the ligands in Cr(III) complexes in aqueous solutions [2].

### 3.3.2.1 Reactivity of *dd* States: Octahedral $Cr^{3+}$ ($d^3$)

The electronic configuration of Cr(III) complexes is $d^3$ ($^4A_{2g}$ in octahedral symmetry). The lowest excited state in these complexes is frequently a *dd*-state ($^4T_{2g}$), formed as a result of a $t_{2g} \rightarrow e_g$ transition with no spin change [25]. This $d \rightarrow d$ transition corresponds to a transition from a non-bonding to an antibonding metal-ligand orbital, hence the metal-ligand bonding is weaker in the excited state, promoting photodissociation and photosubstitution of the ligands.

Octahedral Cr(III) complexes undergo ligand photosubstitution reactions through a variety of mechanisms:

**Photoaquation reactions**:

$$\left[Cr(NH_3)_6\right]^{3+} + H_2O \rightarrow \left[Cr(NH_3)_5(H_2O)\right]^{3+} + NH_3 \qquad (3.1)$$

**Photolabilisation reactions**:

Photolabilisation of the ligand (*i.e.* ligand loss) is believed to be the first step in the light-induced water substitution in the hexa-aqua complex $[Cr(H_2O)_6]^{3+}$. For instance, photolysis of $[Cr(H_2O)_6]^{3+}$ in the wavelength range 400–575 nm in the presence of $Cl^-$ or $SCN^-$ ions lead to a substitution of the water molecule by halogen or pseudohalogen. The quantum yield of this reaction is extremely low—in the order of $10^{-4}$. Such low efficiency corresponds well with the very short lifetime of the excited state, of the order of several picoseconds.

**Photoracemisation reactions:**

Octahedral complexes of three chelating bidentate ligands, LL, can exist as two optical isomers, Δ and Λ. Due to weaker metal-ligand bonding in the excited state, it is possible to induce racemisation photochemically:

$$\Delta - \left[\mathrm{Cr(LL)_3}\right]^{3+} \rightarrow \Lambda - \left[\mathrm{Cr(LL)_3}\right]^{3+} \tag{3.2}$$

These reactions have been studied for a variety of bidentate ligands, including 1,2-diaminoethane, pentane-2,4-dionate, and 1,10-phenanthroline. The quantum yield of the racemisation reaction is of the order of 1–2 % in each case, indicating similar pathways for all of those complexes [2].

### 3.3.2.2 Reactivity of *dd*-States: Rh(III) ($d^6$)

The electronic configuration of octahedral rhodium(III) complexes is low-spin $d^6$. The lowest excited state in these complexes is a *dd*-state, formed as a result of a $t_{2g} \rightarrow e_g$ transition [26]. In contrast to the majority of other transition metal complexes, some Rh(III) complexes have a relatively large energy difference between the *dd*-state and higher lying states of different origin, such as a ligand-to-metal charge transfer (LMCT) state. Therefore the observed photochemistry, if it occurs from the lowest, equilibrated, state is exclusive to the *dd*-state—as confirmed by wavelength-independent photochemistry under excitation within the lowest absorption band manifold. Thus these complexes serve as an excellent model for the ligand field excited state chemistry of other complexes possessing the $d^6$ configuration. Their reactions involve largely ligand dissociation and ligand substitution processes.

$$[\mathrm{Rh^{III}(NH_3)_5Cl}]^{2+} \xrightarrow{h\nu} [dd\text{-state}] \begin{cases} \rightarrow \textit{trans}\text{-}[\mathrm{Rh^{III}(NH_3)_4Cl(Solvent)}]^{2+} + \mathrm{NH_3} \\ \rightarrow [\mathrm{Rh^{III}(NH_3)_5(Solvent)}]^{3+} + \mathrm{Cl^-} \end{cases} \tag{3.3}$$

### 3.3.2.3 Towards Long-Lived Excited States

**Raising the energy of the *dd*-state**

Another, indirect, influence of *dd*-states on photophysics and photoreactivity is through thermal population of a *dd*-state from a lower-lying excited state. The formation of *dd*-states is associated with the large structural distortions due to the Jahn-Teller effect [25]. Consequently, these states provide an efficient channel for non-radiative decay, leading to extremely short excited state lifetimes. For example, thermal population of *dd*-states is held to be responsible for the lack of emission and extremely short (sub-nanoseconds) excited state lifetimes for the lowest metal-to-ligand or ligand-to-ligand excited states (see below) in Pt(diimine)$L_2$ complexes ($L = Hal, PhS^-$ or $RO^-$).

Introduction of strong field ligands raises the energy of the deactivating *dd*-excited states. This is one of the possible strategies to produce highly luminescent complexes, as raising the energy of the *dd*-state implies that an excited state of a different nature—intra-ligand or charge-transfer (see below)—becomes the lowest in energy, and can undergo radiative deactivation to the ground state. Such strategy leads to highly emissive Pt(diimine)(acetylide)$_2$ complexes with the lifetimes up to microseconds in deoxygenated solutions at room temperature (r.t.), if compared to Pt(diimine)Cl$_2$ whose excited-state lifetime is only picoseconds under identical conditions [27]. Thus, introducing a strong ligand-field co-ligand, such as phenyl-acetylide, Ph–C$\equiv$C$^-$, and derivatives achieves the effect of raising the energy of the *dd*-state, thereby removing an important thermally-accessible non-radiative decay pathway and yielding strongly emissive diimine and triimine transition metal complexes [8, 28–31]. Another example is that of the non-emissive [Pt(tpy)Cl]Cl complex, tpy = 2,2′,6′,2″-terpyridine, in which substitution of the terdentate tpy ligand with stronger-field cyclometallating ligands dramatically increased the lifetime and produced new classes of highly emissive complexes (Fig. 3.4). These include N^N^C coordinating ligands, derivatives of 6-phenyl-2,2′-bipyridyl [32], C^N^C ligands [33], or N^C^N type (2,6-dipyridyl-benzene) ligands [34]. The latter ligand type led to a family of Pt(N^C^N)Cl compounds with emission quantum yields of 60–74 % in deoxygenated solution at r.t., and lifetimes up to 8 μs. Such intense and long-lived emission was attributed to a combination of cyclometallating, strong-field, ligands, and the fact that the Pt–C bond is particularly short in this class of compounds in comparison to the N^N^C or C^N^C counterparts, maximising the ligand field effect.

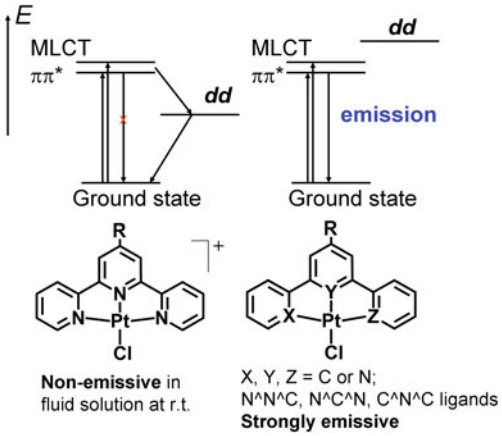


**Fig. 3.4** Tuning the nature of the lowest excited state in Pt(II) chromophores. The charge of the compounds with cyclometallating ligands (*right hand side*) depends on the ligand

**Long-lived intra-ligand excited states**

An alternative route to long-lived excited states in transition metal complexes is to populate an excited state localised on a pendant arm. For example, a switch from a very short lived MLCT state in $[Pt(tpy)Cl]^+$ to a long-lived intra-pyrene excited state in $[(4'\text{-pyrene})\text{-tpy-Pt-Cl}]^+$, has been demonstrated: an electron-rich aryl substituent at the 4′ position of the tpy ligand promotes the low-lying excited state with intra-ligand charge-transfer (ILCT) character, enhances the emission intensity, and extends the excited-state lifetime up to 64 μs in r.t. dichloromethane solution [35].

Another example is that of a Pt(II)-based dyad designed for photoinduced charge separation, $Pt(phen\text{-}NDI)Cl_2$, featuring a naphthalene-1,8-dicarboxy-diimide electron acceptor (NDI) appended to the 1,10-phenanthroline (phen) moiety [36]. Here, an initial excitation producing $^1$MLCT Pt-to-phen excited state is followed by ultrafast ISC into the corresponding $^3$MLCT state, and formation of the charge-separated state $[Cl_2\text{-}Pt^{II}]^{+\bullet}(phen)\text{-}(NDI^{-\bullet})$, which decays partially by reforming the ground state, and partially by populating a $^3$NDI localised excited state which has a lifetime as long as 520 μs.

Yet another interesting instance of achieving a long lifetime—651 μs—of a charge-transfer excited state is a Re(I) complex $Re(PNI\text{-}phen)(CO)_3Cl$, where the PNI-phen is N-(1,10-phenanthroline)-4-(1-piperidinyl)naphthalene-1,8-dicarboximide [37]. Introduction of the PNI-acceptor group increases the lifetime of the $^3$MLCT excited state approximately 3000-fold in comparison to that of the model complex $[Re(phen)(CO)_3Cl]$. The effect was attributed to the thermal equilibration between the emissive $^3$MLCT state and a long-lived triplet state of the $^3$PNI chromophore, which is similar in energy. In this case, the long lifetime was attributed to a specific 'reservoir effect' between $^3\pi\pi^*$ and $^3$MLCT states.

These examples demonstrate the wealth of excited states in metal chromophores and how subtle changes in structure can alter the nature of the lowest excited state and consequently the overall light-induced properties.

### *3.3.3 Metal-Centred Excited States: ff*

Another type of MC transition is *ff*-transitions which occur in lanthanide and actinide complexes. In contrast to *dd*-transitions, much less relaxation of the Laporte selection rule is possible (see Chap. 1), with the result that the molar absorption coefficient for those transitions is typically less than 1–10 $dm^3\ mol^{-1}\ cm^{-1}$. Excitingly, the strongly forbidden nature of the *ff*-transitions has a large positive effect on their photophysical properties—the emission emanating from *ff*-excited states is extremely long lived, which makes lanthanide complexes most attractive candidates for any emission–related applications, from sensing to imaging of live cells to pressure detectors and optoelectronics, of which the most well-known are the Nd:YAG laser and the phosphors used in 'fluorescent' lights and cathode-ray tube television screens [2]. The lability of the Ln/Ac metal–ligand bonds leads to a

wealth of thermal substitution reactions, and, consequently, photochemical ligand substitution is rarely studied. The main photochemical reactions of interest in the complexes of the lanthanide and actinide ions are photoredox reactions.

The photochemistry of lanthanide complexes typically concerns the ligands, and in most cases does not involve metal-centred redox process. The main exceptions are redox couples $Eu^{2+/3+}$, $Yb^{2+/3+}$ and $Ce^{3+/4+}$, in which the reactions are driven by increased stability of $Ce^{4+}$, $Eu^{2+}$, $Yb^{2+}$ and due to the empty ($4f^0$) half-filled ($4f^7$) or filled ($4f^{14}$) electronic configurations respectively.

## *3.3.4 Charge Transfer Transitions*

The charge transfer (CT) transitions discussed below are characterised by:

1. moderate to large molar absorption coefficients, from $\sim 10^2$ to $\sim 10^4$ $dm^3\ mol^{-1}\ cm^{-1}$;
2. the energy of the transition being dependent on the donor/acceptor properties of the ligands involved;
3. the corresponding absorption and emission bands do not show vibrational progression;
4. negative solvatochromism of the corresponding absorption band for the majority of CT transitions, whereby the energy of the transition decreases with the decrease in the polarity of the solvent [4].

### 3.3.4.1 Metal-to-Ligand Charge Transfer

This type of transitions is common when the metal centre has a relatively low oxidation potential, and a relatively low-lying vacant molecular orbital is localised on the electron-accepting ligand. Thus, the metal centre acts as an electron donor, and the ligand as an electron acceptor, to give a charge-transfer $M^{\bullet+}$–$L^{\bullet-}$ excited state with an oxidised metal centre and a reduced ligand. Typical examples include diimine complexes of transition metals, such as Ru(II), Re(I) or Pt(II).

The archetypal example of the compound which possesses an MLCT lowest excited state, formed as a result of a light-induced shift of electron density from the metal centre to the ligand, is the tris(bipyridyl)Ru(II) dication, $[Ru(bpy)_3]^{2+}$. The structure and the schematic energy level diagram for this ion are given in Fig. 3.5.

The $[Ru(bpy)_3]^{2+}$ dication efficiently absorbs light in the visible region ($\lambda_{max} = 452$ nm, $\varepsilon = 13{,}000\ dm^3\ mol^{-1}\ cm^{-1}$ in acetonitrile), forming an $^1$MLCT excited state. This process is followed by rapid intersystem crossing to the lowest triplet ($^3$MLCT) state, facilitated by strong spin–orbit coupling associated with the

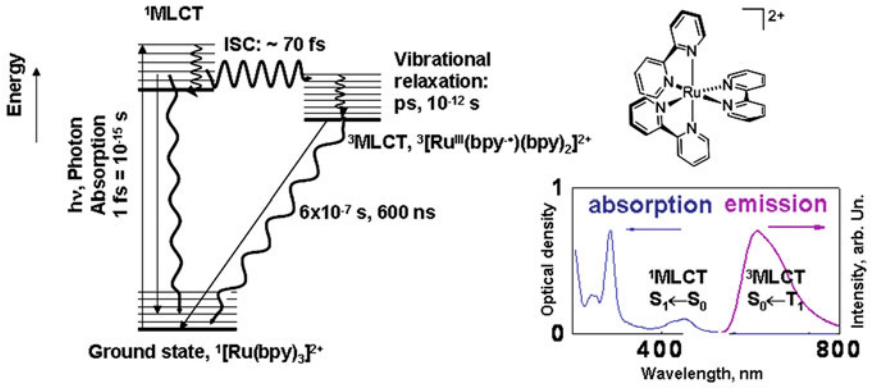


**Fig. 3.5** Structure of the octahedral $[Ru(bpy)_3]^{2+}$ ion, the corresponding energy level diagram showing the major processes and their time scales, and the absorption/emission spectra of $[Ru(bpy)_3](PF_6)_2$ in hexane at r.t

Ru-centre. The rate of intersystem crossing to the $^1$MLCT state is of the order of hundreds of femtoseconds or even faster [38, 39]. As emission from the $^3$MLCT excited state to the singlet ground state is spin-forbidden, it has a relatively long lifetime in deoxygenated solutions at r.t. (e.g. 630 ns in water) [40]. The relatively high emission quantum yield (2.8 % in aerated water) has led to its use as an emission standard.

The long lifetime of the $^3$MLCT state, and the relative ease of its reduction and oxidation, make this complex a useful model for the studies of photoinduced electron transfer. As a result of such a favourable combination of photophysical properties, numerous artificial photosynthetic systems have been constructed based on this complex both as a chromophore and as an electron donor or acceptor in its excited state. Whilst the ion is photochemically inert at r.t., photolysis of its aqueous solution at 95 °C with 436 nm irradiation results in labilisation of 2,2′-bipyridine [40]. It was therefore proposed that a different, reactive excited state becomes accessible at higher temperatures. This upper state lies $\sim$3600 cm$^{-1}$ (0.44 eV) higher in energy than the lowest state, and is assigned to a *dd*-state, which gives rise to ligand substitution photochemistry.

A well-developed series of complexes with rich MLCT excited-state behaviour are Re(I)-diimine complexes. $[Re(bpy)(CO)_3Cl]$ was the first transition metal complex used as a catalyst for $CO_2$ reduction to CO, proposed by Lehn and Ziessel [41]. This series of complexes is particularly amenable to study of the excited state by time-resolved infrared spectroscopy. Formation of the $^3$MLCT Re $\rightarrow$ bpy excited state leads to a reduction of the electron density on the metal centre. Consequently, $d \rightarrow \pi$ backbonding from Re *d*-orbitals to the antibonding $\pi^*$ orbitals of CO ligands is reduced, resulting in an increase of the energy of the stretching vibrations, $\nu$(CO), by several tens of wavenumbers in the excited state if

compared to the ground state. This large effect allowed the researchers to follow the dynamics of the charge transfer process by monitoring the rates of formation and decay of the transient bands in the infrared spectrum.

### 3.3.4.2 Ligand-to-Metal Charge Transfer

This type of transition occurs from an occupied, low-lying ligand-localised orbital to a vacant orbital of the metal centre. It is most common if the metal centre is highly oxidised, and the ligand is a strong electron donor (*i.e.* the exact converse of the situation which gives rise to MLCT excited states). A classical example is the permanganate anion $MnO_4^-$, in which an intense violet–purple color is due to an LMCT transition. Whilst $MnO_4^-$ is formally a *d*-metal complex, no *dd*-transitions can take place in a fully oxidised Mn(VII) centre that has the $d^0$ configuration.

The uranyl ion, $UO_2^{2+}$, provides another example of an LMCT state, this time involving *f*-orbitals of the metal centre [42]. The LMCT excited state, which is the lowest excited state, is formed by electron transfer from a *p*-orbital of the uranyl oxygen atom to an empty 5*f*-orbital on the uranium centre, giving rise to intense absorption at *ca.* 420 nm. An intriguing property of the $UO_2^{2+}$ is its phosphorescence that emanates from the lowest triplet state with a potential quantum yield of 100 % in the solid state. The chemistry and photochemistry of the uranyl cation has seen a recent renaissance, largely inspired by its relevance to nuclear waste monitoring and processing. A variety of luminescent adducts have been developed (Fig 3.6, left) [43], which can potentially be used for emission sensing in the environment and/or in extraction and reprocessing conditions.

An LMCT is also the lowest transition of some Mo-dithiolene complexes which are used as components in various magnetic and conducting materials and in chemical analogues of the catalytic centres of molybdenum oxo-transferase enzymes such as sulfite oxidase and DMSO reductase [44]. Also, many Mo-dithiolene complexes, including [$(Cp)_2$Mo(dithiolene)] compounds (Fig. 3.6, right), possess not one but several dithiolene-Mo LMCT transitions close in energy to one another due to the presence of several closely-spaced and energetically accessible vacant *d*-orbitals on the Mo centre [45].

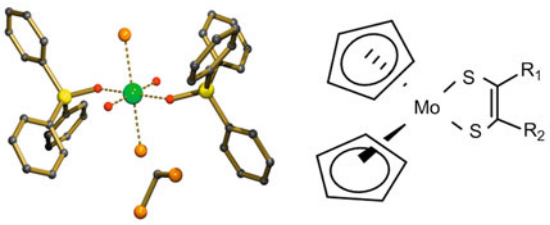


**Fig. 3.6** Examples of compounds with a lowest energy LMCT excited state. *Left*-$UO_2$-adducts trans-$UO_2Cl_2(OAsPh_3)_2$ [43], *right*-Mo$(Cp)_2$(dithiolene) [45]

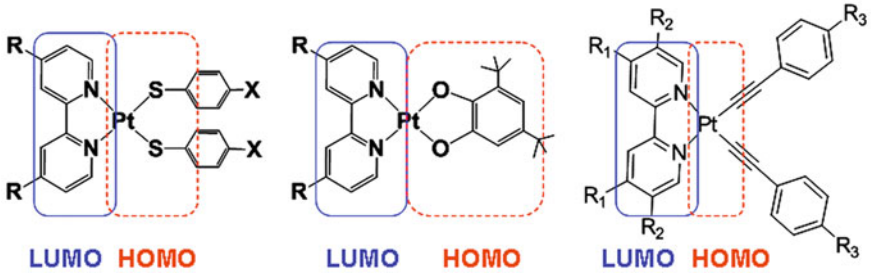


**Fig. 3.7** Different types of charge-transfer transitions in Pt(II) diimine complexes bearing thiolate, catecholate, or acetylide donor ligands

### 3.3.4.3 Ligand-to-Ligand Charge Transfer

This type of electronic transition occurs if one of the ligands has a high-lying occupied orbital, and another has a low-lying vacant orbital, such that one is a good electron donor and the other a good electron acceptor. In most cases the orbitals involved cannot be classified as 'pure' ligand-localised orbitals, but have some degree of metal character. Thus the usual notation is not LLCT, but ML′/LLCT for this type of transition, which is a more correct reflection of the orbital composition. Of course the transition probability depends on an overlap between the orbitals involved, and hence metal *d*-orbital contribution in both the highest occupied molecular orbital (HOMO) and the lowest unoccupied molecular orbital (LUMO) increase significantly the extinction coefficient of such electronic transitions.

Pt(diimine)(dithiolate) [46], Pt(diimine)(thiolate)$_2$ or Pt(diimine)(catecholate) complexes (Fig. 3.7) are typical examples of the compounds possessing lowest electronic transition of mainly LLCT nature, from thiolate/catecholate (HOMO) to diimine $\pi^*$ (LUMO). The absorption maxima, emission maxima and oxidation potential of these compounds dramatically depend on the donor ligand. For example, the oxidation peak potential for Pt(2,2′-bipyridine)(4-X-$C_6H_4$-S)$_2$ compounds changes from +0.58 V for X = $NO_2$, to –0.23 V for X = $NMe_2$ (*vs* $Fc^+$/Fc in THF), whereas the 1st reduction potential is almost not affected. Such a strong influence of the thiolate ligand on the oxidation potential of the complex clearly indicates its significant participation in the HOMO [47]. However, even in this case there is a considerable contribution of Pt *d*-orbitals in both the HOMO and the LUMO, and thus the excited state is a combination of MLCT/LLCT, denoted {charge-transfer-to-diimine}, or ML′/LLCT lowest excited state.

The extent of the contribution of the Pt *d*-orbitals to the frontier orbitals can be directly assessed by electron paramagnetic resonance (EPR) (spectro) electrochemical experiments as demonstrated in Fig. 3.8. These experiments are only possible for those compounds in which the redox process in question is chemically and electrochemically reversible. For example, the EPR studies on the radical anions revealed ~10 % contribution of Pt(II) orbitals in the LUMO of Pt(4,4′-$X_2$-2,2′-bipyridine)$Cl_2$ systems [48]. Likewise, 12 % Pt $d(z^2)$ contribution in the

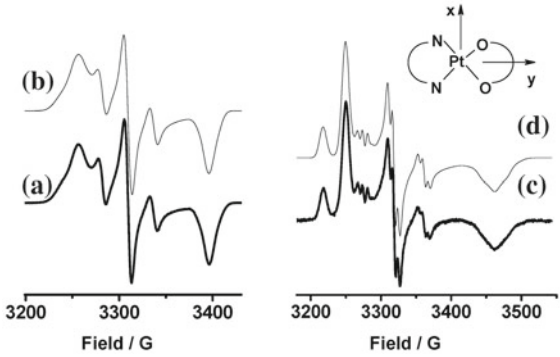


**Fig. 3.8** Pt($^t$Bubpy)($^t$Bucat)cation (*left*) and anion (*right*). Experimental **a** and simulated **b** EPR spectra of radical-cation in $CH_2Cl_2$ containing 0.4 M $[Bu_4N][PF_6]$ at 77 K. Experimental **c** and simulated **d** EPR spectra of 1 the radical-anion in DMF containing 0.2 M $[Bu_4N][PF_6]$ at 77 K. Copyright ®American Chemical Society 2008 [49]

HOMO was determined by modelling the EPR spectra of the radical-cation of the complex [Pt(2,9-$Ph_2$-1,10-phenanthroline)(catecholate)], and of related compounds [49]. Participation of metal-based orbitals in the HOMO and the LUMO is significant for photophysical properties—it leads to higher molar absorption coefficients ($\sim 10^3$ $dm^3$ $mol^{-1}$ $cm^{-1}$) than for a transition which is purely LLCT in nature, such as the one observed in the analogous tetrahedral Zn(diimine)$(SAr)_2$ complexes where the LLCT is 'pure' with $\varepsilon \sim 200$ $dm^3$ $mol^{-1}$ $cm^{-1}$ [50].

The solvatochromic behaviour of the absorption spectra of complexes of this type illustrated in Fig. 3.9 is a further proof of the charge-transfer nature of the lowest electronic transition. Differently to thiolate or catecholate complexes, the lowest excited state in the bis-acetylide complexes Pt(diimine)$(C\equiv C\text{-}R)_2$ ($R = 4\text{-}X\text{-}C_6H_{4-}$) mentioned above is a charge-transfer from the largely Pt based HOMO to the Pt/diimine-based LUMO. Consequently, the effect of electron donating properties of the acetylide ligand has much lesser influence on the redox and optical properties of the complexes [29, 30, 51] if compared to thiolate ligands.

### 3.3.4.4 Sigma-Bond-to-Ligand Charge Transfer

Another type of CT transition is that resulting in sigma-bond-to-ligand charge transfer states, also known as $\sigma$–$\pi^*$ states. Those involve an occupied orbital located on a sigma-bond between the metal centre and a ligand, and a vacant orbital located on the ligand. Examples of compounds with a SBLCT excited state are the metal–metal bonded compounds $[M(SnR_3)_2(CO)_2(\alpha\text{-diimine})]$ (M=Ru, Os; R=Me, Ph) [52, 53] (Fig. 3.10). The SBLCT transition is accompanied by a shift of electron density from the $\sigma$(Sn–M–Sn) bonding orbital to the $\alpha$-diimine-ligand. Consequently, the SBLCT excited states often undergo a photo-induced M–Sn

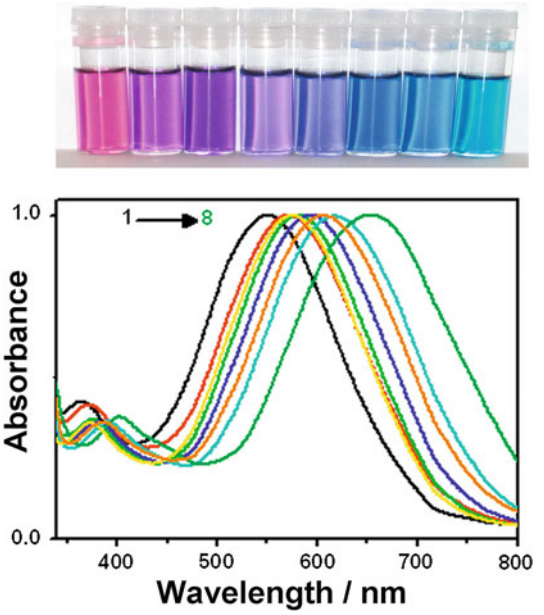


**Fig. 3.9** The LLCT lowest absorption band, and its solvatochromism, for Pt(bpy)(3,5-di-$^{t}$Bu-catecholate). Normalised absorption spectra recorded in solvents of different polarity: *1* methanol, *2* ethanol, *3* $CH_3CN$, *4* DMSO, *5* DMF, *6* acetone, *7* $CH_2Cl_2$, and *8* $CHCl_3$ Adapted with permission from Ref. [15]. Copyright 2010 American Chemical Society

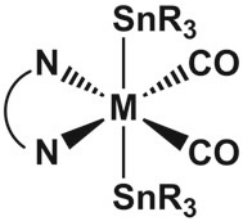


**Fig. 3.10** Sigma-bond-to-ligand charge transfer is exemplified in $[M(SnR_3)_2(CO)_2(diimine)]$ (M = Ru, Os; R = Me, Ph)

bond homolysis at room temperature and provide an example of dissociative photochemistry, which in turn opens up routes to new compounds.

The selected examples above demonstrate the wealth of excited states in metal chromophores and how subtle changes in structure can alter the nature of the lowest excited state and consequently the overall light-induced properties.

### 3.3.5 Tuning the Nature of the Lowest Excited State by the Nature of the Ligand

The presence of a manifold of close in energy low-lying excited states of different origin is an intrinsic feature of transition metal complexes. This feature opens up exciting possibilities to tune their photophysical properties as well as their photoreactivity by modifying the ligand(s).

A series of octahedral complexes $[Re^{I}X(CO)_3(bpy)]$ (X = halide) and related Ru(II) complexes provide an illustration of this idea. The lowest excited state in $[Re(Cl)(CO)_3(bpy)]$ is of primarily Re → bpy MLCT character, although the HOMO has some $Cl^-$ contribution. Upon replacement of $Cl^-$ with $Br^-$, and further with $I^-$, the HOMO gains an increasingly larger contribution from the halide anion, and the lowest excited state gradually becomes a halide(X) → ligand (bipy $\pi^*$) charge-transfer (XLCT) [54]. A similar trend is observed for the nature of the lowest excited state in complexes $[RuX(Me)(CO)_2(diimine)]$ (diimine = bpy; R-DAB: *N*,*N*-di-R-1,4-diaza-1,3-butadiene) along the sequence X = Cl, Br, I.

These complexes also demonstrate a change in the excited state character between a Frank-Condon (vibrationally 'hot') electronically excited state and the vibrationally relaxed, lowest excited state. Resonance Raman (rR) spectra show that the vibrationally hot Franck–Condon states of $[RuI(Me)(CO)_2(i\text{Pr-DAB})]$ have virtually pure XLCT character [55]. However, the TRIR data indicate that thermally equilibrated, vibrationally-relaxed excited state has a mixed MLCT–XLCT character [6]. Hence, combining the results from resonance Raman and TRIR data allows one to obtain insight into charge redistribution processes in the excited state on a very short timescale.

The nature of the lowest excited state in Pt(II) diimine complexes Pt(diimine)$X_2$ can also be tuned by the nature of the ligands—and is shifted from largely Pt → bpy MLCT (for X = Cl), to a ML'/LLCT excited state for X = $ArS^-$.

The diversity of excited state types and how they can be tuned by the nature of the ligand is also very well illustrated by metal–metal and metal–alkyl bonded diimine complexes of Re, Ru, Pt and Os. The photochemistry and photophysics of those complexes varies dramatically with the change of the ligands, as the nature of the lowest excited state changes from a long lived SBLCT state in $Ru(SnPh_3)_2(CO)(i\text{Pr-DAB})$ (DAB = 1,2-diazabutadiene) which has a strong Ru-Sn bond, to dissociative in $Pt(alkyl)_2(diimine)$, to very reactive SBLCT-ones in the case of $Re(SnR_3)(CO)_3(diimine)$ (with formation of radicals) or triangular clusters such as $Os_3(CO)_{10}(diimine)$ (which generates biradicals and zwitterions). We will return to some of those examples later in the Chapter.

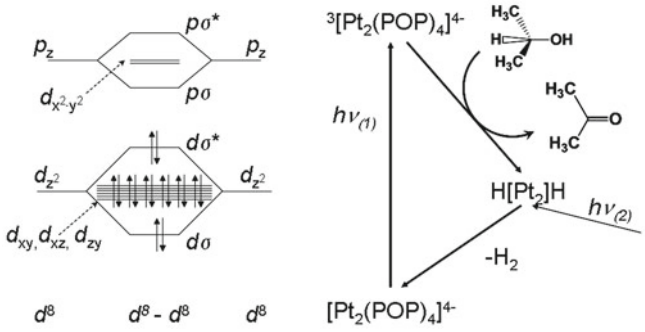


**Fig. 3.11** *Left* molecular orbital diagram of $[Pt_2(P_2O_5H_2)_4]^{4-}$; *Right* Dehydrogenation of isopropanol to acetone using $[Pt_2(P_2O_5H_2)_4]^{4-}$ as a photocatalyst, based on the description in [6]

### *3.3.6* Some Dimetallic Species

The excited states of dinuclear $d^8$–$d^8$ platinum, rhodium, and iridium complexes with a variety of bridging ligands exhibit unusually diverse reactivity. These types of compound in their lowest triplet state engage in oxidative and reductive electron transfer reactions, and exciplex formation [56]. They can also engage in atom transfer reactions: *i.e.* they can abstract hydrogen atoms from a wide range of substrates as well as halogen atoms from alkyl and aryl halides.

The most widely documented diplatinum(II) complex is $[Pt_2(P_2O_5H_2)_4]^{4-}$, which contains bridging (P,P-bonded) diphosphito ligands (Figs. 3.11, 3.12). Photophysical studies confirm that the properties of the photoactive excited state are a manifestation of $d^8$–$d^8$ metal–metal interactions [57].

*Excited-state atom transfer: Halogens and H*

The triplet state of $^3[Pt_2(POP)_4]$ is quenched by halogen atom transfer reagents such as alkyl and aryl halides. It also reacts with hydrogen-atom donors—alcohols, $Bu_3SnH$, $Et_3SiH$, or $H_3PO_3$ [57]. The first example of C–H bond cleavage by $[Pt_2(P_2O_5H_2)_4]^{4-}$ was the photochemical conversion of isopropyl alcohol to acetone and hydrogen (Fig. 3.11). The first step is hydrogen atom abstraction of the methine hydrogen, yielding the radical pair $\{[Pt_2(P_2O_5H_2)_4]^{4-}\text{-H}\}^{\bullet}$ and $(CH_3)_2COH^{\bullet}$. This photoinduced reaction is a two-electron process, is catalytic in $[Pt_2(P_2O_5H_2)_4]^{4-}$, and has been shown to occur *via* a triplet excited state (Fig. 3.11).

There is no formal metal–metal bond in the ground electronic state of these bimetallic compounds. However, light absorption promotes an electron from the antibonding $d\sigma^*$ to the bonding p$\sigma$ ($p_z$-derived) orbitals, creating a partial (formal order of one) metal–metal bond in the excited state [56]. This transient bonding determines the photophysical and photochemical properties of these complexes. The ultrafast intersystem crossing in the initially formed $^1d(\sigma^*)p(\sigma)$ state yields a corresponding triplet state, which, after thermal equilibration, persists for microseconds.

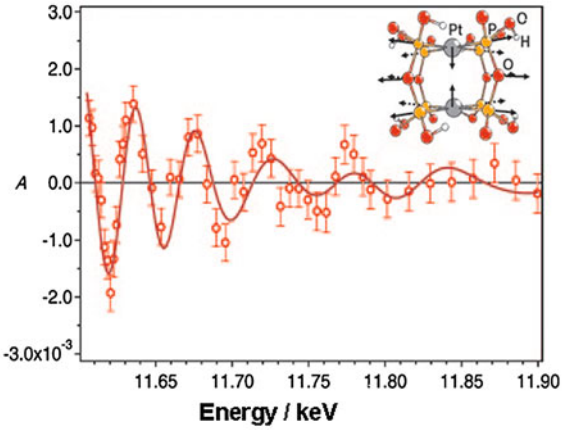


**Fig. 3.12** Photoinduced structural changes in $[Pt_2(P_2O_5H_2)_4]^{4-}$ in solution obtained from EXAFS studies. Transient data (*circles*) and best fit (*solid line*) were obtained with the following parameters: a Pt–Pt contraction of 0.31(5) Å, a Pt–ligand elongation of 0.010(6) Å, zero energy shift, and 7 % excitation yield. The error bars represent the standard error of the measurement. *Red circles* oxygen, *orange circles* P, *grey circles* Pt, *small white circles* H atoms. Adapted with permission from Ref. [59]. Copyright 2009, John Wiley & Sons

Since the reactivity is largely occurring form this lowest triplet state, it is important to directly determine its structure. Recently, a large contraction of the Pt…Pt bond in the triplet excited state of $[Pt_2(P_2O_5H_2)_4]^{4-}$ has been confirmed directly by time-resolved X-ray diffraction [58] and pico-nanosecond X-ray absorption [59] spectroscopy (Fig. 3.12) and DFT calculations [60]. The results suggest that the strengthening of the Pt–Pt interaction is accompanied by a weakening of the ligand coordination bonds, resulting in an elongation of the platinum–ligand bonds, as schematically shown in the inset in Fig. 3.12.

### *3.3.7 Multiple Metal–Metal bonds*

Another type of excited state arising in multinuclear metal systems is the $\delta\delta^*$ excited state [61–64]. This occurs in quadruply–bonded dinuclear complexes, such as $[Re_2Cl_8]^{2-}$ or $[M_2X_4(PR_3)_4]$ where M=Mo or W. In contrast to $[Pt_2(P_2O_5H_2)_4]^{4-}$ described above, this type of compound possesses a strong—quadruple—bond between two metal centres in the ground electronic state, with the overall electronic configuration of $\sigma^2\pi^4\delta^2$. This bonding is weakened by a promotion of electron density to the antibonding, $\delta^*$, orbital in its lowest $\delta \rightarrow \delta^*$ electronic excited state. An interesting feature of these compounds is that in the initially studied, phosphate-supported $M_2$-systems the singlet $^1\delta \rightarrow \delta^*$ excited state is longer lived than its triplet counterpart, $^3\delta \rightarrow \delta^*$. The reason for this

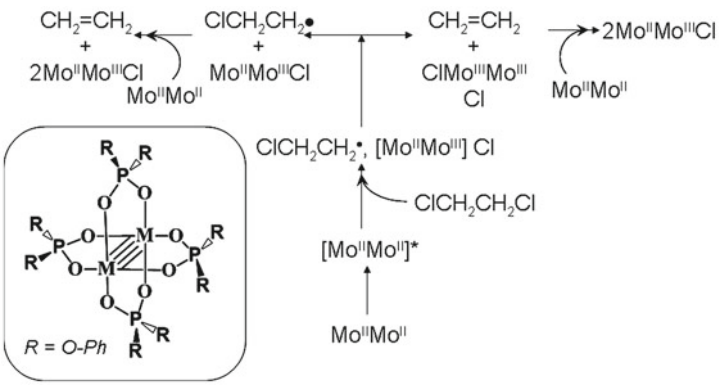


**Fig. 3.13** Proposed mechanism of the photochemical reduction of 1,2-dichloroethane by $Mo_2(O_2P(OC_6H_5)_2)_4$, adapted from [64]

behaviour is two-fold: firstly, the $S_1 - T_1$ splitting is very large, and secondly, the $T_1$-$S_0$ splitting is relatively small, as manifested by the emission occurring in the NIR range of the spectrum. The small $T_1$-$S_0$ splitting promotes non-radiative deactivation due to higher density of overlapping vibrational states, which can be described in terms of the energy gap law (Chap. 1) [65].

The presence of two metal centres opens up the possibility to study electronic coupling, and for multielectron photoredox processes to take place, whilst relatively long lifetimes of the excited states (see below) makes possible bimolecular reactions in solution. Accordingly, quadruply-bonded di-Re complexes have been reported to engage in bimolecular electron-transfer reactions, whereas the di-Mo and di-W complexes participate in oxidative addition and two-electron redox reactions. For example, UV irradiation of phosphate-supported $M_2$ dinuclear complexes under acidic conditions leads to one- or two-electron oxidation of the metal–metal core accompanied by production of $H_2$ gas by reduction of two protons.

A further example of multielectron photooxidation is that of $[Mo_2\{PO_2(OC_6H_5)_2\}_4]$ (Fig. 3.13). The lowest energy absorption maximum in this compound occurs at 515 nm in dichloroethane ($\varepsilon = 156$ dm$^3$ mol$^{-1}$ cm$^{-1}$) and corresponds to the formation of a $^1\delta \rightarrow \delta^*$ excited state, whose lifetime of 68 ns is sufficiently long to engage in bimolecular reactions in solution at r.t. Irradiation of this compound with visible light ($> 500$ nm) in 1,2-dichloroethane led to formation of ethene, whilst the two Cl atoms from a solvent molecule undergo oxidative addition to the two Mo centres. The maximum quantum yield (0.040) for this reaction is observed upon irradiation at 510 nm, confirming that the reactivity originates from the $^1\delta \rightarrow \delta^*$ state whose absorption maximum is in this region [64].

These $M_2$ complexes offer ample opportunities for tuning their photophysical and photochemical properties by the change of the metal and the supporting ligands. This property is well illustrated by the quadruply bonded dicarboxylates of M=Mo or W, $[M_2(O_2CR)_4]$, in which the $[M_2(O_2CR)_4]$ core has a paddle-

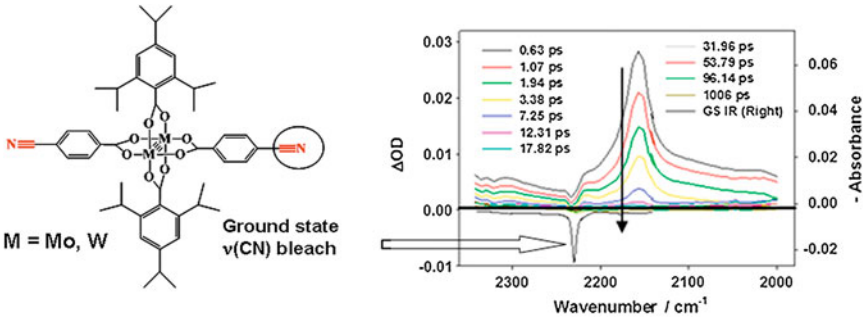


**Fig. 3.14** Ultrafast time resolved infrared spectroscopy of a $Mo_2$-system supported by carboxylate-type ligands (*left*) in THF at r.t. The spectra are interpreted as a delocalised $^1$MLCT excited state at early times, which fully decays into $^3\delta\delta^*$ excited state (lifetime < 10 ns), not detectable in this experiment. Reprinted with permission from Ref. [67]. Copyright © 2011 the National Academy of Sciences

wheel arrangement and local $D_{4h}$ symmetry [66]. In contrast to the phosphinate-supported dinuclear systems described above, these carboxylate-supported systems possess a low-energy $^1$MLCT transition due to the low-lying $\pi^*$ orbital of the carboxylate unit, $\{\sigma(M_2) \rightarrow \pi^*(CO_2)\}$. The energy of this transition can be tuned across the entire visible and NIR region of the spectrum, from 400 nm to 1000 nm, by changing the metal (Mo *vs* W) and involving different conjugated R-groups. Thus interplay between singlet and triplet MLCT and $\delta \rightarrow \delta^*$ excited states is possible. These $M_2$ complexes frequently exhibit dual emission, demonstrating the presence of several weakly interacting excited states. The fluorescence from these compounds is typically solvent-dependent, pointing towards a charge-transfer nature of the emitting state, *i.e.* $^1$MLCT. On the contrary, phosphorescence from the majority of $Mo_2$–containing compounds is solvent independent, and is also relatively unaffected by the nature of the carboxylate ligand. It occurs at ~1100 nm and possess a long emission lifetime of 10–100 μs; this indicates that the emitting, lowest triplet state for $Mo_2$-carboxylate-supported compounds is a $^3(\delta \rightarrow \delta^*)$ one, associated with the MoMo bond. Therefore there is the possibility to change the relative order of MLCT *vs* $\delta \rightarrow \delta^*$ excited states by changing the design of the compound and thus controlling the reactivity [66–68].

An important question with respect to the structure and the nature of the reactive excited state(s) in such species is whether it is a localised or a delocalised state(s), and what is the time scale of the intersystem crossing?

These questions have been recently addressed using ultrafast time-resolved infrared spectroscopy (Fig 3.14), on the example of *trans*-$M_2(T\mathit{i}PB)_2(O_2CC_6H_4$-4-$CN)_2$, where T*i*PB is 2,4,6-triisopropyl benzoate, which has an IR-reporting CN group. Figure 3.14 shows an example of the TRIR spectra for M=Mo. The bleach of the stretching vibration $\nu$(CN) in the ground state, at 2239 $cm^{-1}$ is clearly seen. Notably, the IR bands in the excited state are much broader, and more intense than

that of the ground state. Such behavior is indicative of the large delocalisation in the excited state [66, 67].

Thus, the TRIR studies indicated that in *trans*-$M_2(T\mathit{i}PB)_2(O_2CC_6H_4\text{-}4\text{-}CN)_2$ the $S_1$ state is delocalised over a *trans* pair of carboxylate ligands, and is $^1$MLCT in nature for both Mo and W complexes. The lowest triplet excited state in the $W_2$-compounds was assigned as $^3$MLCT [67]. In contrast, in the $Mo_2$ analogue the long-lived triplet states ($\sim$50 μs) is $^3\delta \rightarrow \delta^*$ in nature. This excited state is not detectable by TRIR as it results in no significant changes in the CN stretching vibrations, but is detectable with transient absorption studies.

These differences in the nature of the lowest excited state arise from the balance between the relative orbital energies of the $M_2(\delta)$ or $M_2(\delta^*)$ and the ligand $\pi^*$ orbitals, as well as the magnitudes of the orbital overlap. Such differences in the nature and the degree of delocalisation between singlet and triplet excited states, fine-tuned by ligand design in a set of structurally similar $M_2$ compounds, demonstrates the breadth of excited states and associated potential reactivity in quadruply-bonded complexes.

One practical application lies in molecular photonics, where incorporation of the $M_2$ units into conjugated oligomers and polymers could allow for the optical properties and conductivity to be modulated by the properties of the $M_2$ unit [68].

## 3.4 Dissociative Photochemistry

The majority of ligand-dissociation reactions are thought to occur on the ultrafast time scale. A relatively rare case of a 'slow' ligand dissociation from a relaxed excited state takes place in some amino complexes of Rh(III) and Ir(III), or in Co(II) polycyano complexes. In these complexes, the lowest ligand-field (*dd*) state is formed upon $t_{2g} \rightarrow e_g$ excitation, and undergoes ligand dissociation and consequent ligand substitution reaction on a nanosecond time scale.

### *3.4.1 Ligand loss: Dissociation of CO in Metal Carbonyls*

Metal carbonyl complexes provide an important advantage for large-scale chemical synthesis due to the high efficiency of the carbonyl ligands' dissociation under photo-excitation, or at elevated temperatures. Accordingly, metal carbonyl compounds have been extensively used as catalysts in organic syntheses and in catalytic industrial processes [69]. Moreover, recently metal carbonyl complexes have been incorporated into photochromic materials, with applications such as logic gates, information storage or optical switches in mind [7].

The photochemistry of classic examples of transition metal carbonyls—such as $Cr(CO)_6$, $W(CO)_6$ or $Fe(CO)_5$—demonstrates the diversity of reaction pathways and potential products. The labilisation of CO and replacement by another ligand

is the most common photoreaction of mononuclear metal carbonyls $M(CO)_x$ [70]. Detailed spectroscopic studies of the photoreaction intermediates in low temperature matrices [71], and early studies in solutions [72] have shown that in most cases the first step in this reaction is monomolecular dissociation. The dissociation product can be easily solvated by an even weakly coordinating solvent, which can be replaced should a 'trapping ligand'—a stronger coordinating moiety—be present in solution, thus forming a new compound.

$Ni(CO)_4$—the first metal carbonyl compound, discovered in 1890 [73]—and $Fe(CO)_5$, which was discovered the following year, are the two most studied metal carbonyl compounds [74]. In particular, the photochemistry of $Fe(CO)_5$ has been extensively studied due to its widespread use in industrial processes as a cheap and reactive compound utilised in a variety of applications, from polymerisation to metallurgy. Consequently, there has been great interest in the mechanisms of reactions, and especially the initial photochemical processes, occurring in $Fe(CO)_5$ upon irradiation under ambient conditions [75]. Initially, such photochemical studies were only possible in low temperature matrices, in which reactive intermediates would be 'trapped' and interrogated by infrared spectroscopy. Several key intermediates such as $^3Fe(CO)_4$ and $Fe(CO)_3$ have been identified.

The development of ultrafast methods has allowed the study of the photochemistry of $Fe(CO)_5$ in solutions at r.t. The photochemical mechanisms thus became accessible, and, for example, the elusive species $Fe(CO)_3$ and the conversion between $\{^3Fe(CO)_4\}$ and $\{^1Fe(CO)_4(solvent)\}$ has been observed in heptane solution and in supercritical (sc) fluids, such as $scCH_4$ or scXe [76].

Another classic example of a ligand loss reaction is the ultrafast [77] dissociation of CO from $Cr(CO)_6$, with the formation of the pentacarbonyl $Cr(CO)_5$, which occurs with a lifetime of less than 100 fs:

$$Cr(CO)_6 \rightarrow Cr(CO)_5 + CO \tag{3.4}$$

$Cr(CO)_5$ is only observable in the gas phase at reduced pressure; this $16e^-$ species is extremely reactive and engages in an assortment of processes to complete its coordination sphere—dimerisation yielding dimetallic species, or ligand coordination, leading to a variety of products in the gas and liquid phase.

The nature of the dissociative excited state is still being discussed. For instance, for $Cr(CO)_6$, the dissociative excited state was initially believed to be a *dd*-state; however, calculations by DFT and TD-DFT methods indicated that the lowest excited state may have a Cr-to-CO MLCT character.

In a similar fashion, photolysis of $W(CO)_6$ leads to CO loss, and the resulting species $W(CO)_5$ persists in weakly coordinating solvents such as heptane. However, addition of a coordinating solvent such as THF to the heptane leads to fast (diffusion-controlled) formation of the corresponding THF complex:

$$W(CO)_6(h\nu) \rightarrow W(CO)_5 + CO \rightarrow W(CO)_5(THF) \tag{3.5}$$

If the reaction is performed in THF, but in the presence of an even stronger coordinating ligand L, such as pyridine, THF may also be replaced:

$$W(CO)_5(THF) + L \rightarrow W(CO)_5L \tag{3.6}$$

For instance, photolysis of $W(CO)_6$ in benzene and cyclohexane in the presence of L = py or $CH_3CN$ occurs with a quantum yield of 0.7, which is independent of the excitation wavelength in the range from 254 to 366 nm, and also independent of the concentration of the coordinating ligand L [78]. These early observations pointed towards a dissociative mechanism of photosubstitution, in accordance with the subsequently established ultrafast nature of the CO-dissociation.

Monosubstituted metal carbonyls $M(CO)_5L$ can react with another coordinating ligand $L^1$ *via* two principal dissociative pathways: initial CO loss and subsequent formation of $[M(CO)_4LL^1]$), or initial loss of the ligand L followed by formation of $M(CO)_5L^1$. The balance between the two pathways is determined by the nature of the ligand L. For example, for M = W, when L is a nitrogen-donor ligand such as acetonitrile or pyridine, the lack of back-donation from the ligand to M-CO bond increases the bond strength (as is also reflected in the $\nu$(CO) values), making the M-CO bond dissociation unfavourable and thus encouraging the L-loss pathway. If L = phosphine, the L-loss and the CO-loss pathways have similar quantum yields of 0.3 [79]. This type of reaction is the gateway to a very wide range of organometallic compounds.

Other metal carbonyls—for example those of Ru or Re—are less photolabile, however, in some cases CO dissociation can also occur. For example, irradiation at 365 nm of *fac*-$[Re(X_2bpy)(CO)_3(PR_3)]^+$ leads to photoinduced CO loss and its replacement with the coordinated solvent molecule, $CH_3CN$:

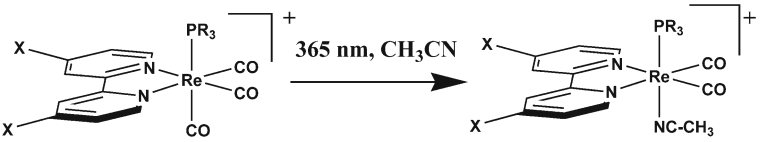


(3.7)

Metal carbonyls are capable of photoactivating small molecules, such as $N_2$, $H_2$, or alkanes. In this context, studies of high pressure reactions in polyethylene films have demonstrated the versatility of the photochemistry of $Fe(CO)_5$, in which one of the CO-ligands could be photochemically replaced by $N_2$ or $H_2$, whilst the thermal reaction of $Fe(CO)_4(N_2)$ with $H_2$ demonstrated the higher stability of the $H_2$-complex (Fig. 3.15) [80].

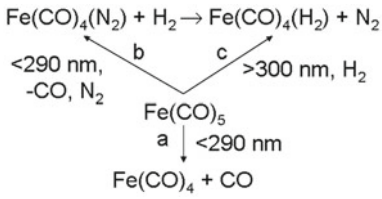


**Fig. 3.15** Photochemical ligand substitution in $Fe(CO)_5$ [80]

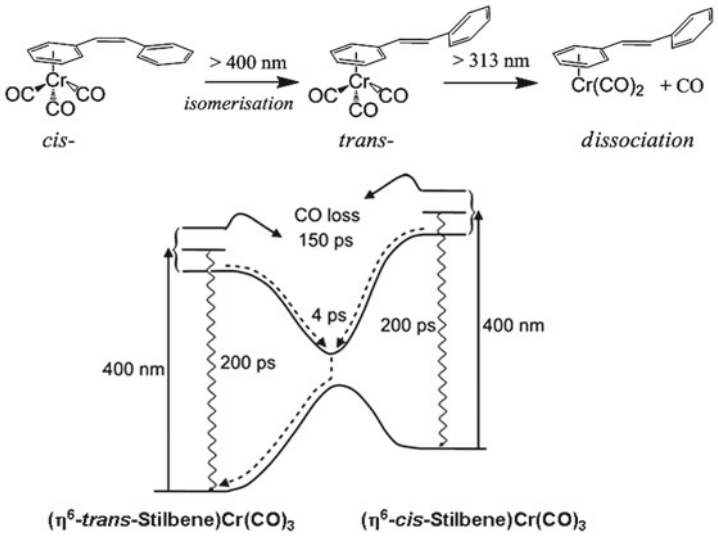


**Fig. 3.16** Wavelength-dependent photochemical transformations in a Cr carbonyl complex. Reprinted with permission from Ref. [86]. Copyright 2007, American Chemical Society

For binuclear metal carbonyls, $M_2(CO)_{2X}$, the photophysics and photoreactivity are strongly affected by the presence of a metal–metal bond and of a bridging carbonyl ligand. The CO-dissociation is still of course possible, however, a M–M bond cleavage is also taking place, producing $17e^-$ species:

$$Mo_2(CO)_{2X} \rightarrow 2Mo(CO)_X \text{ or } \left\{Mo_2(CO)_{2x-1} + CO\right\} \tag{3.8}$$

The ratio of the products is usually wavelength-dependent. Their subsequent reactions will be determined by the coordinating ability of the solvent, and by other species present in solution, all of which will compete with recombination and reformation of the starting material.

For example, in the photochemistry of $Mn_2(CO)_{10}$ the balance between initial formation of $^{\bullet}Mn(CO)_5$ (by cleavage of the Mn–Mn bond) and $Mn_2(CO)_9$ (by dissociation of CO) is wavelength dependent. Irradiation with 355 nm light populates selectively the lowest $\sigma \rightarrow \sigma^*$ transition, leading to the Mn–Mn bond cleavage and the ratio between the two pathways being 0.74. On the other hand, irradiation with 266 nm light populates a metal-to-CO $\pi^*$ antibonding orbital, leading to CO dissociation, and the ratio of the two pathways becomes 0.21, with formation of $Mn_2(CO)_9$ dominating [81]. It is interesting to note the potential for photochemically selective reactions: for example, selective CO loss has been achieved in mixed dinuclear species, e.g. $MnRe(CO)_{10}$, studied using matrix isolation and time-resolved infrared spectroscopy [82].

Photoinduced CO loss frequently competes with other possible photochemical pathways. The example of Cr(stilbene)$(CO)_3$ photochemistry demonstrates

wavelength-dependent photo-transformations (Fig. 3.16). Irradiation with >400 nm light leads to photoisomerisation *via* population of an intermediate MLCT excited state. On the other hand, irradiation with 313 nm light leads to CO loss, *via* an MC-state, and formation of a solvent adduct.

Apart from fundamental interest in photochemistry of metal carbonyls, there is considerable interest in therapeutic applications of carbon monoxide release to physiological targets [83]. A photo-activated 'pro-drug' which would release CO only upon irradiation would be a good option for CO delivery. One of the challenges for such applications is to create water soluble complexes. A photoactivated carbon monoxide releasing moiety, $[W(CO)_5(L)]^{3-}$ has been designed, which is an air-stable, water-soluble tungsten(0) carbonyl complex of the trianionic ligand L = tris(sulphonatophenyl)phosphine. Near-UV photolysis of this compound in an aqueous buffer solution leads to release of a single CO molecule with high quantum yield (Eq. 3.9). Furthermore, in aerated media, additional CO is slowly released from the $[W(CO)_4(H_2O)(L)]^{3-}$ photoproduct owing to autoxidation of the tungsten centre. Thus this water-soluble complex serves as a carbon monoxide releasing moiety both in the primary photochemical reaction and in the secondary reactions of the initially formed photoproduct [83].

$$W(CO)_5(L)^{3-} \xrightarrow[H_2O]{h\nu} W(CO)_4(H_2O)(L)^{3-} + CO \qquad k_{CO} \tag{3.9}$$

The carbonyl complex salt $Na_3[W(CO)_5(L)]$ is very stable in aerated aqueous media unless subjected to photolysis. Under irradiation, this compound demonstrates high photolability, leading to the release of approximately one CO. Nuclear magnetic resonance (NMR) data confirm that phosphine photolabilisation is at most a minor pathway (<5 %), making $Na_3[W(CO)_5(L)]$ an effective photoactivated carbon monoxide releasing moiety for possible pharmaceutical applications [83].

### *3.4.2 Ligand Loss: NO*

Many transition metal nitrosyl complexes release NO upon photolysis. For example, NO release was observed from Mo(CO)(NO)(dppe)(dtc), where dtc = $S_2CNMe_2$, and dppe = diphenyl-phosphino-ethane. The lowest energy absorption band of this compound, at 520 nm, has been assigned to a LLCT (dtc → $NO^*$) transition. Photolysis into the low energy side of this band ($\lambda_{irr}$ = 546 nm) in benzene solutions results in loss of NO ($\phi$ = 0.0018) [84].

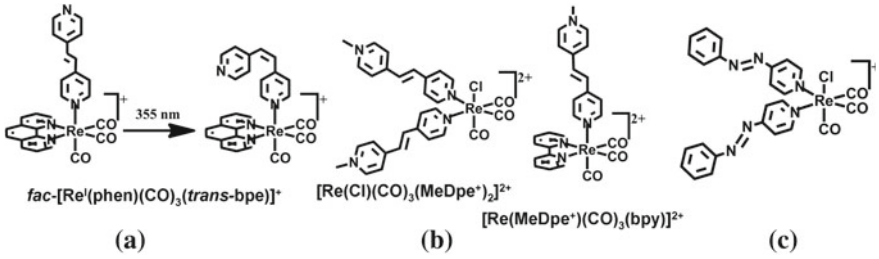


**Fig. 3.17** Examples of *cis–trans* ligand isomerisation on a metal centre initiated by light

### *3.4.3 Photoinduced cis–trans Isomerisation*

*Cis–trans* photoisomerisation in organic molecules is a well-studied process. Photoisomerisation of alkenes and azobenzenes forms a basis for applications ranging from information storage to molecular motors [3]. Usually, due to absorption properties of the organic compounds, UV light is required to initiate photoisomerisation. Attachment of the photoisomerisable units to transition metals opens up a route to use low energy, non-destructive visible light to initiate isomerisation *via* CT states.

For instance, *cis–trans* isomerisation in stilbene is one of the most studied isomerisation processes in organic compounds. It occurs efficiently using 313 nm irradiation. An example of a stilbene-type *cis–trans* isomerisation on a metal centre was reported for Re(I) [85]. In this example, the process occurs under UV light, and time-resolved infrared studies provided direct evidence for a ligand-based photochemical transient (Fig. 3.17a).

However, attachment of a $Cr(CO)_3$ moiety to one of the benzene rings in *cis*-stilbene [86] has shown that the complex [*cis*-($\eta^6$-stilbene)$Cr(CO)_3$] efficiently undergoes photoisomerisation to the *trans* isomer following irradiation with light longer than 400 nm (Fig. 3.16) [7].

Isomerisation on the Re(I) centre of a stilbene analogue bearing instead of two Ph-groups two quartenised pyridine groups—$[Re(Cl)(CO)_3(MeDpe^+)_2]^{2+}$ and $[Re(MeDpe^+)(CO)_3(bpy)]^{2+}$ (bpy = 2,2-bipyridine, $MeDpe^+$ = *N*-methyl-4-[trans-2-(4-pyridyl)ethenyl]pyridinium)—has been investigated (Fig. 3.17b). Studies of the excited state dynamics of these complexes have clearly demonstrated how photoprocesses can be controlled by changes in structure. Whilst $[Re(MeDpe^+)(CO)_3(bpy)]^{2+}$ isomerises following photoexcitation, its bipyridine-free analog $[Re(Cl)(CO)_3(MeDpe^+)_2]^{2+}$ does not. It was proposed that excitation of $[Re(MeDpe^+)(CO)_3(bpy)]^{2+}$ at 400 nm leads to population of *both* $Re(CO)_3 \rightarrow MeDpe^+$ and $Re(CO)_3 \rightarrow$ bpy $^3$MLCT states, both of which rapidly convert to a $MeDpe^+$ localised intraligand $^3\pi\pi^*$ excited state ($^3$IL) in $< 600$ fs, and $< 10$ ps, respectively. The product containing *cis*-isomer of the $MeDpe^+$ ligand is then formed from this $^3$IL state. In the case of the $[Re(Cl)(CO)_3(MeDpe^+)_2]^{2+}$ complex the lowest excited state is assigned to a $Re(Cl)(CO)_3 \rightarrow MeDpe^+$ $^3$MLCT.

This state decays to the ground state with lifetimes of <42 and 430 ps without isomerisation, indicating that the $^3$IL state can not be populated [87].

Another well-studied example of *cis–trans* isomerisation is that of azobenzene and derivatives (Fig. 3.17c). Similarly to the stilbenes described above, an attachment of the azobenzene derivative as a ligand to the transition metal centre allows photoisomerisation of azobenzene by using lower energy light than is needed for the free ligand.

Photoisomerisation on a metal centre can alter emission properties of the complexes, or even result in an on/off emission switch, and accordingly this type of reactions has been explored for sensing applications [88].

It is important to reiterate that the timescales of many of the processes discussed above are ultrafast—picoseconds or even sub-picoseconds—and therefore these reactions occur from a non-equilibrated, vibrationally hot electronic exited state(s).

### *3.4.4 Photoinduced Linkage Isomerism*

Thermally activated linkage isomerism in solution has been known since the time of the pioneering work of Alfred Werner (Nobel prize in Chemistry, 1913). Recognition of *photoinduced* linkage isomerism came only a few decades ago, and since then a very large number of transition metal complexes have been shown to undergo this inner-sphere photoreaction. Ligands susceptible to this process are *ambidentate*, *i.e.* they have the potential to coordinate in more than one way. Examples of ligands engaging in linkage isomerism include: nitrosyl ligand –NO coordinating *via* either the N or the O atoms; nitro-ligand with N *vs* O coordination, $-SO_2$ and dimethyl-sulfoxide (DMSO) ligands with S *vs* O atom coordination, isocyanate (N *vs* S donor), and some others. Linkage isomerism can be used as a synthetic tool to obtain a particular isomer in a pure form, but is also important technologically, in relation to potential photorefractive applications, including data storage and optical switching, as well as logic gates [89, 90].

Initially, this process was studied using low temperature methods, involving matrix isolation and IR spectroscopy, as the two linkage isomers would have very different IR spectra and frequently exhibit a change in the energy of the ligand stretching vibration of over 100 $cm^{-1}$ upon isomerisation. For example, $\nu$(NO) in *cis*-$[RuCl(en)_2NO]Cl_2$ shifts from 1901 to 1775 $cm^{-1}$ between the two forms in which NO is coordinated *via* the N atom or the O atom [89].

In recent years, the investigation of photoinduced linkage isomerism has become intrinsically linked to the new method of photocrystallography [17]. Photocystallography is a rapidly developing technique that enables the full three-dimensional structure of a molecule, in a crystalline environment, to be determined by X-ray crystallography when the molecule has been photoactivated into a short-lived excited state. Similarly, X-ray absorption (XAFS) can be used to provide structural details of excited state molecules in the solid state or in solution. In the

**Fig. 3.18** Fully reversible nitro–nitrito linkage isomerismLinkage isomerism in a single crystal, in $-NO_2$-containing complex of Ni(II), [Ni($Et_4$dien)($\eta^2$-O,ON)($\eta^1$-$NO_2$)]. Ni turquoise, N *blue*, O *red*; $Et_4$dien = *N*,*N*,*N*′,*N*′-tetraethyldiethylenetriamine. Copyright ®John Wiley & Sons 2011 [96]

solid state, photocrystallography has achieved the crystallographic characterisation of species with sub-microsecond lifetimes [18, 91, 92].

Amongst the examples above, linkage isomerism is particularly common in nitrosyl containing compounds—a recent review stated that out of over 100 nitrosyl coordination compounds studied, about 80 % showed evidence of N/O linkage isomerism [89]. Examples include [Ni(NO)($\eta^5$-Cp*)], a wide variety of Ru(II) complexes, e.g. *cis–trans*-[RuCl($en)_2$NO]$Cl_2$ or *trans*-[RuCl(NO)$Py_4$]$PF_6$, and Mn(CO)$(NO)_3$.

Light-induced linkage isomerism has been documented in, for example, $Na_2$[Fe$(CN)_5$NO], upon excitation into the lowest absorption band assigned to a Fe($d\pi$) → NO($\pi$*) MLCT transition [93]. The presence of two light-induced metastable states was indicated by Mossbauer spectroscopy, and their structural characterisation was performed in the late 1990s by photocrystallography [92]. Despite being a common occurrence, the linkage isomerism of nitrosyl compounds occurs only at low temperatures, and with very low yields, under the experimental conditions used.

Practical applications exploiting reversible switching between linkage isomers would require photostability, and 100 % reversible isomerisation at ambient temperature and pressure. The factors affecting the interconversion process have been the subject of intense study, and recent work [94] has shown that the excited state potential must possess a minimum close to the saddle point of the ground state energy surface between the ground and metastable states, or cross that surface, so that relaxation from the excited state into the metastable minima can occur. The first fully reversible single-crystal-to-single-crystal isomeric interconversion was observed in the nitrite complex [Ni(dppe)(Cl)$(NO_2)$] at temperatures below 160 K [95]. A very recent example demonstrates fully reversible nitro–nitrito linkage isomerism in a single crystal, in an $-NO_2$-containing complex of Ni(II), [Ni($Et_4$-dien)($\eta^2$-O,ON)($\eta^1$-$NO_2$)] (Fig. 3.18). The N-bound $NO_2$ group in this complex has been shown to undergo reversible conversion into the O-bound nitrito linkage isomer under both thermal and photoactivation of a single crystal. Photocrystallographic studies were undertaken on the slow-cooled clean nitro-($\eta^1$-$NO_2$) isomer,

by irradiating the crystal *in situ* for a period of 1 h at 100 K. The subsequent X-ray data set showed that a photochemical linkage isomerisation reaction had occurred with 86 % of the crystal converted into the nitrito-($\eta^1$-ONO) isomer [96].

Linkage isomerism in sulfoxide complexes is also a rather frequent phenomenon [90]. Some metal sulfoxide complexes can exist in both S-bonded and O-bonded metastable states. The isomerisation can occur with high yields, at room temperature, and in solutions as well as in the solid state, as has been demonstrated for a wide variety of Ru(II) and Os(II) complexes. For example irradiation of [Ru(tpy)(Me-pic)(DMSO)]$^+$, with 413 nm light (corresponding to the MLCT transition) yields sulfur → oxygen (S/O) isomerisation of the DMSO ligand with a quantum yield of 0.79. Amongst many other examples are [Ru(bpy)(tpy)(DMSO)]$^{2+}$ and [Ru(bpy)$_2$(DMSO)$_2$]$^{2+}$ in which the quantum yield of isomerisation varies considerably with changing from tpy to bpy ligands [90]. The S/O linkage isomerisation is believed to occur *via* temporary oxidation of Ru(II) to Ru(III); accordingly, it can be promoted either electrochemically, or photochemically *via* an MLCT state. Recent ultrafast optical spectroscopic studies are indicative of a $^3$MLCT state being the key intermediate state in the isomerisation of Ru(II) complexes, whereas for [Os(bpy)$_2$(DMSO)$_2$]$^{2+}$ the transient absorption studies indicate that a higher-lying CT state is the intermediate state.

Linkage isomerism of DMSO in Ru(II) poly-pyridyl complexes has been used as a synthetic tool to access enantio-pure complexes such as [Ru(bpy)$_2$(DMSO)Cl]$^+$ [97]. The mechanism of the isomerisation and the nature of the excited states involved continue to be investigated by a variety of means, including picosecond transient absorption spectroscopy and modern crystallographic methods.

### 3.4.5 Photoinduced Isomerisation at the Metal Centre, Within the Coordination Sphere

Labilisation of the ligands can cause rearrangement of the positions of the ligands within the coordination sphere of a metal complex, without changing its composition. One of the first examples is the *cis–trans* isomerisation of [Ru(bpy)$_2$(H$_2$O)$_2$]$^{2+}$ (Fig. 3.19, left) under irradiation with visible light [98]. The quantum

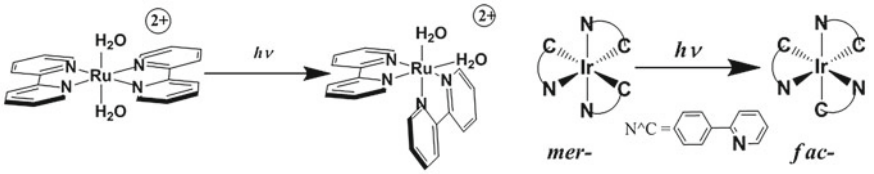


**Fig. 3.19** Photoisomerisation in the coordination sphere. *Left*: *cis–trans* isomerisation of Ru(II) complex; *Right*: *mer/fac* isomerisation of an Ir(III) complex with three cyclometallating ligands, such as 2-phenyl-pyridine

yields for *cis-trans* and *trans–cis* isomerisations are wavelength-independent, suggesting that the process occurs from the lowest electronic excited state in each case.

Another possible type of coordination isomerisation is that observed for octahedral complexes of the type $MA_3B_3$, or bearing three bidentate chelating ligands whose donor atoms are inequivalent. Such compounds can exist as facial (*fac*) or meridional (*mer*) isomers, and photoinduced transformation between the two is possible in some cases. Highly emissive complexes of Ir(III) with cyclometalating chelating ligands such as 2-phenylpyridine undergo such a transformation (Fig. 3.19, right). These compounds are highly luminescent, and are used in various light-related applications, from cell imaging to organic light-emitting diodes (OLEDs). A change from a *fac-* to *mer-* arrangement of the ligand set alters the photophysical properties of the complex (the *fac*-isomer is considerably more emissive) and as such this reaction is directly related to the performance and durability of the compounds in a particular application [99].

### 3.4.6 Reductive Elimination

Photochemical reductive elimination offers further examples of ultrafast light-induced reactions. Irradiation of *cis*-$[Ru(dmpe)_2H_2]$ with 300 nm light in cyclohexane causes elimination of $H_2$, and rearrangement of the $[Ru(dmpe)_2]$ 'skeleton' (dmpe—$Me_2P\text{-}CH_2\text{-}CH_2\text{-}PMe_2$) to the *trans* isomer. Interestingly, all of those processes were reported to be completed within the instrument response time of 16 ps [100].

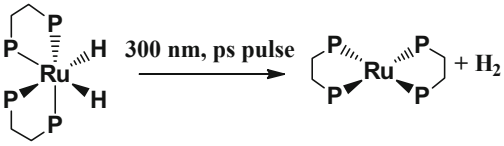


(3.10)

### 3.4.7 Oxidative Addition

The conversion of alkanes into more useful products is one of the most important practical problems in chemistry. The insertion of metals into C–H bonds was first discovered by Chatt and Davidson in 1965 [101] for low-valent ruthenium complexes. Following the discovery of the photochemically induced insertion of a transition metal into alkane C–H bonds [102, 103], a large number of organometallic complexes have been shown to activate C–H bonds in alkanes. A typical example is the photochemical oxidative addition of alkanes to complexes such as $Rh(Cp)(CO)_2$. The reaction occurs *via* an initial loss of CO followed by $\sigma$-

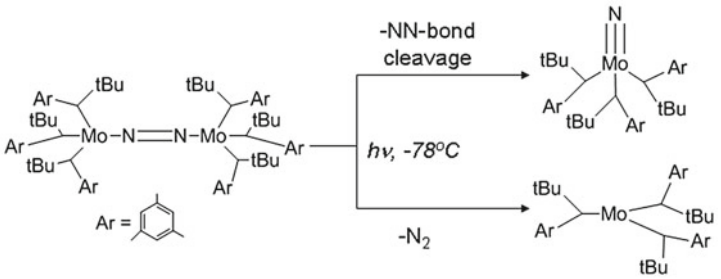


**Fig. 3.20** Dinitrogen splitting with Mo complexes [105]

coordination of the alkane. A wide diversity of products can be obtained using this type of transformation.

$$\mathrm{Rh(Cp)(CO)_2} \xrightarrow{hv,\ alkane} \mathrm{Rh(Cp)(CO)(alkane)} \rightarrow \mathrm{Rh(Cp)(CO)(H)(alkyl)} \qquad (3.11)$$

## 3.5 Photoactivation of Small Molecules with Transition Metal Complexes

### *3.5.1 Dinitrogen Splitting*

Activation of the most stable molecule—$N_2$—is another major challenge in chemistry. The difficulty originates from the extreme stability of the triply-bonded $N_2$ with the bond energy of the $N \equiv N$ bond being extremely high, 944 kJ $mol^{-1}$. A photochemical route to $N_2$ activation is an attractive option as it can potentially overcome this difficulty, providing the required energy through photoexcitation. Accordingly, photochemical studies of $N_2$-bridged metal complexes with the aim of $N_2$-splitting have been reported, although the number of such studies at present is very limited.

Photochemical NN bond cleavage has been realised in a linear, bimetallic Mo-mesityl complex (Mes = 2,4,6-$Me_3C_6H_2$-), which led to formation of a $\mu$-nitride-product as well as dinitrogen [104]:

$$(\mu\text{-}N_2)\left[\mathrm{Mo(Mes)_3}\right]_2 \rightarrow (\mu\text{-N})\left[\mathrm{Mo(Mes)_3}\right]_2 + 0.5\ N_2 \qquad (3.12)$$

In a related example, a dimolybdenum $N_2$-bridged complex was found to undergo competitive $N_2$ elimination and –NN-bond cleavage under photolysis into the lowest energy absorption band with 544 nm light. The presence of two different products (quantum yield = 0.05 with respect to the starting compound) was confirmed by a variety of methods including $^{15}N$ NMR spectroscopy and X-ray crystallography to isolate the product of $N_2$-elimination (Fig. 3.20) [105].

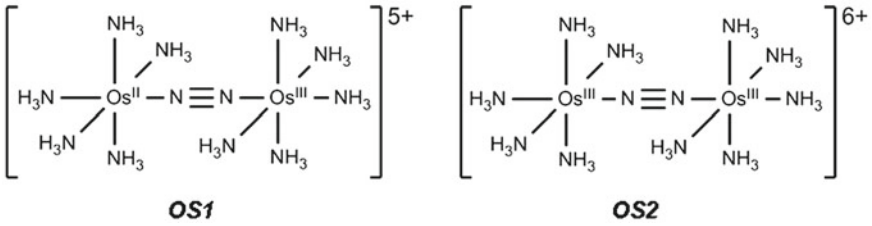


**Fig. 3.21** Diosmium complexes of dinitrogen [106]

In the examples above, the reactivity of the –N=N- unit was exploited. A recent example discusses an $N_2$-bridged Os dimer in which the –NN-bridge largely preserves its triple bond character. It demonstrates how homoleptic $N_2$-splitting can be achieved photochemically with the use of Os complexes, as well as how tuning of the nature of the lowest excited state can dramatically alter the photochemical properties and the nature of the reaction products [106].

The mixed-valence complex OS1 (Fig. 3.21), which contains Os(II) and Os(III) centres bridged by a dinitrogen ligand, exhibits two main bands in the absorption spectrum: 700 nm ($\varepsilon = 4000\ \mathrm{dm^3\ mol^{-1}\ cm^{-1}}$) due to an intervalence $Os^{II} \rightarrow Os^{III}$ transition and 238 nm ($\varepsilon = 41000\ \mathrm{dm^3\ mol^{-1}\ cm^{-1}}$) due to an MLCT transition $Os^{II}[d(\pi)] \rightarrow N_2(\pi*)$

Because of the different nature of those transitions, different photochemical products are formed depending on the excitation wavelength. Excitation into the inter-valence transition at 700 nm does not initiate any photoreactivity. However, irradiation with light <450 nm populates an MLCT state, resulting in transient oxidation of the metal centre, reduction of the $N_2$ molecule, and dinitrogen splitting, with quantum yields 0.002 and 0.003 under 254 nm or 365 nm irradiation respectively.

$$\left[(NH_3)_5Os^{II}(\mu\text{-}N_2)Os^{III}(NH_3)_5\right]^{5+} \rightarrow 2\left[Os^{VI}(NH_3)_4N\right]^{3+} + 2NH_3 + e^- \quad (3.13)$$

Notably, compound OS1 is also an interesting example of a violation of Kasha's rule, *i.e.* the higher lying excited state does not simply convert quickly to the lower-lying one, but the two have independent and quite different reactivity (Fig. 3.21).

In sharp contrast with OS1, compound OS2 does not cleave dinitrogen. Instead, it evolves $N_2$ gas, and, whilst the compound is somewhat thermally unstable and slowly releases nitrogen even without irradiation, photolysis causes violent evolution of $N_2$. The difference between the reactivity of OS1 and OS2 can be explained by differences in the energies of their MLCT states: the MLCT ($Os^{III} \rightarrow N_2$) is considerably higher in energy than $Os^{II} \rightarrow N_2$ MLCT, and is not accessible with light >230 nm. Instead, *dd*-states (ligand field, intra-Os) become the lowest energy excited states, and the corresponding *dd*-transition can initiate $N_2$-elimination instead of $N_2$-cleavage.

### 3.5.2 Solar Energy Conversion: Water Splitting and Reduction of $CO_2$

Owing to their strong light absorbing properties and diverse photoreactivity, many transition metal complexes have been utilised in research towards solar energy conversion—ranging from light-harvesting and efficient photoinduced charge separation, to dye-sensitised solar cells, and photovoltaics. Photocatalytic applications cover the whole spectrum of reactions, including $H_2$ production, water splitting, and $CO_2$ reduction towards value added products. There are exciting developments in this vibrant field [6, 7, 107] which are covered in more detail in Chap. 7.

## 3.6 Clusters

Many photoinduced reactions in organometallic chemistry start from organometallic clusters. The most widely used definition is that a cluster is a polynuclear complex consisting of three or more transition metal atoms, connected to one another by direct metal–metal bonds [108].

Cluster chemistry has been an area of intense interest over recent decades due to its relevance to the surface catalysis and interaction of small molecules with metal surfaces, their own catalytic capabilities, and a presence of multimetallic redox centres relevant to biological systems [109].

The clusters can be classified into two main types—so-called 'naked' clusters which do not have stabilising ligands, and those which do involve ligands. Clusters of main group elements typically carry hydride as a stabilising ligand. Most common stabilising ligands in transition metal clusters are CO, halides and pseudohalides, alkenes, and hydrides.

In general terms, based on the formal oxidation state of the metal and electron donating/accepting properties of the ligands, two main sub-categories of transition metal clusters can be identified:

1. Clusters of the group V–VII metals in high formal oxidation states, stabilised by $\pi$-donor ligands such as oxide, sulphide, or halides. Examples here include $[Nb_6Cl_{12}]^{4+}$, $[W_6Br_8]^{4+}$and $[Re_3Cl_9]^{3+}$.
2. Clusters of transition metals in formal low oxidation states, stabilised by $\pi$-acceptor ligands, such as carbonyl or phosphine. Example include many clusters of Os, Mn, Re, Ru, or Fe.

Examples of the smallest clusters, consisting of only 3 metal atoms, are $[Os_3(CO)_{12}]$ or $[Ru_3(CO)_{12}]$. An increase in the number of metal atoms brings about a variety of geometries, such as tetrahedral $[Co_4(CO)_{12}]$, octahedral $[Rh_6(CO)_{16}]$, and proceed further to the large clusters, such as $[Pt_{24}(CO)_{30}]^{n-}$ (n = 0 to 6).

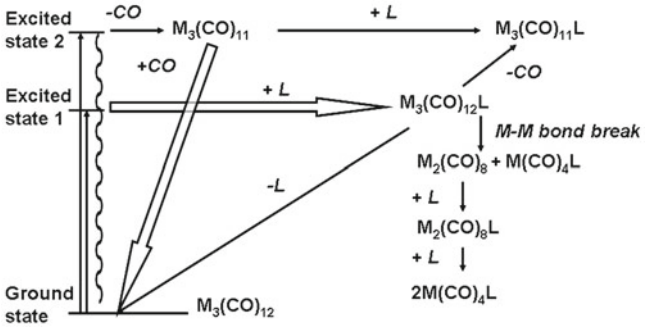


**Fig. 3.22** Possible photoinitiated reactions of clusters $M_3(CO)_{12}$, M = Fe(0), Os(0), Ru(0), in the presence of a coordinating ligand L [111]

The primary photochemical reactions of transition metal clusters include:

1. homoleptic metal–metal bond cleavage with the transient formation of a biradical;
2. heteroleptic metal–metal bond cleavage and formation of a zwitterion;
3. CO dissociation, frequently accompanied by a –CO-bridge formation (the first direct observation of a CO-bridged primary photoproduct of $[Ru_3(CO)_{12}]$ was achieved by picosecond TRIR spectroscopy) [110].

Further reactions of these initially-formed transient species and the relative quantum yield of each pathway depend partly on the coordination ability of the solvent and the reagents, and partly on the nature of the metal involved (Fig. 3.22) [111].

We will briefly consider the photochemistry of transition metal carbonyl clusters, which contain metal centres in low oxidation states and are stabilised by $\pi$-accepting CO ligands. Such transition metal carbonyl clusters are valuable synthetic precursors in both thermal and photochemical synthesis.

As discussed above, the primary process in monometallic carbonyl complexes is CO loss, whilst in dinuclear compounds, $M_2(CO)_{2X}$, there is a possibility of either CO loss, or M–M bond dissociation. In molecular clusters, the photophysics and photoreactivity are significantly different from that of $M(CO)_X$ due to electronic delocalisation across the multi-metallic core.

### *3.6.1 Photochemistry of $[M_3(CO)_{12}]$ in Solution, M = Fe, Ru, Os*

Some of the best known mixed-metal clusters are group VIII triangular clusters $[M_3(CO)_{12}]$ (M = Fe, Ru, Os) [111–113], where almost all possible metal combinations have been prepared [114, 115], and their bonding properties, electrochemistry and photochemistry have been studied in much detail [111–117].

The presence of several low-lying excited states in $[M_3(CO)_{12}]$ clusters gives rise to wavelength-dependent photochemistry, as exemplified for M = Os. Similarly to the binuclear species discussed above, excitation with light at wavelengths longer than 400 nm populates the lowest ($\sigma-\sigma^*$) excited state, and initiates M–M cleavage, resulting in photo-fragmentation and formation of a variety of mono- and dinuclear species—$M(CO)_5$, $M_2(CO)_3L$ and others. High-energy excitation, at wavelengths <350 nm, populates an antibonding, $\pi^*$ M-CO orbital, initiating CO loss and subsequent substitution by coordinating ligands. The observation that the photoreactions under high energy excitation do not occur from the lowest excited state (*i.e.* Kasha's rule is not obeyed) once again indicates that CO loss is likely to occur on the ultrafast time-scale, from a vibrationally hot, non-equilibrated excited state.

$$Os_3(Co)_{12} \underset{1-\text{octene}}{\overset{h\nu(436\,\text{nm})}{\rightarrow}} Os\,(CO)_4(\eta^2-1-\text{octene}) + OS_2(CO)_8(\mu-\eta^1,\ \eta^1-1-\text{octene}) \tag{3.14}$$

$$Os_3(Co)_{12} + P(OEt)_3 \underset{Os}{\overset{h\nu(436\,\text{nm})}{\rightarrow}} 3(CO)_{11}(P(OEt)_3) + CO) \tag{3.15}$$

$$Os_3(Co)_{12} \underset{-CO}{\overset{h\nu(<300\,\text{nm})}{\rightarrow}} Os_3(CO)_{11} \xrightarrow{+L} Os_3(CO)_{11}L \tag{3.16}$$

### *3.6.2 α-Diimine-Containing Clusters*

Replacement of two CO ligands with a diimine ligand to give $[Os_3(CO)_{10}$(diimine)] profoundly changes the photochemical properties compared to the parent cluster $[Os_3(CO)_{10}]$. The lowest excited state in a variety of those clusters has largely an MLCT (Os-to-diimine) character with some degree of $\pi$-delocalisation within the [Os-diimine] moiety, as shown by resonance Raman spectroscopy. This transition gives rise to the absorption band in visible region of the spectrum.

These diimine clusters demonstrate solvent-dependent photochemistry (Fig. 3. 23) [118]. Zwitterions $[^{-}Os(CO)_4\text{-}Os(CO)_4\text{-}Os^{+}\text{-}(S)(CO)_2(\text{diimine})]$ are formed in coordinating solvents (S) such as acetonitrile, whilst irradiation in non-coordinating solvents such as toluene leads to homoleptic cleavage of the metal-meta bond and formation of biradicals $[^{\bullet}Os(CO)_4\text{-}Os(CO)_4\text{-}\{Os^{+}(CO)_2(\text{diimine})^{\bullet-}\}]$. The zwitterions are formed with quantum yields of $\sim 0.01$, and have lifetimes of seconds in nitrile solvents, and even longer (minutes) in pyridine; they mainly regenerate the parent cluster when they collapse. The lifetimes of the biradicals are considerably shorter, and vary from 5 ns to 1 μs, depending on the nature of the diimine ligand. In a minor reaction pathway, the biradicals can isomerise into a diimine-bridged Os-diimine-Os dimer. It is interesting to note that the photoproducts observed—biradical, zwitterions,

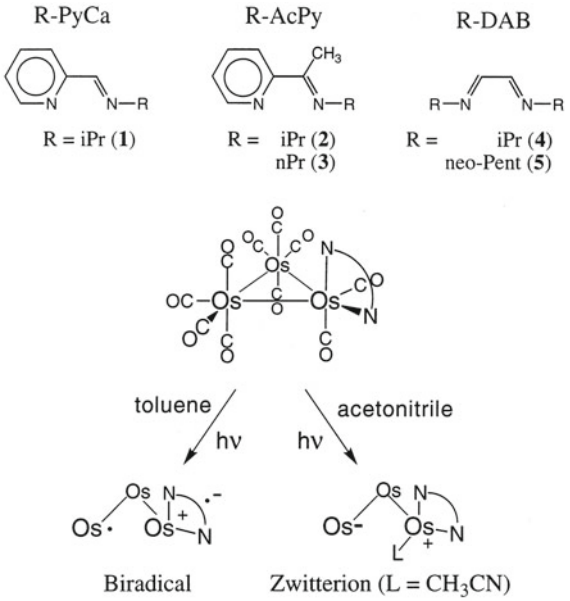


**Fig. 3.23** Schematic structures of the $Os_3(CO)_{10}$(diimine) clusters, of their zwitterions and biradicals, and of the diimine ligands used: R-PyCa = pyridine-2-carbaldehyde *N*-alkylimine; R-AcPy = 2-acetylpyridine *N*-alkylimine; R-DAB = N,N′-dialkyl-1,4-diaza-1,3-butadiene. Copyright ®American Chemical Society 1998 [121]

and diimine-bridged dimers—are similar to the binuclear, metal–metal bound complexes such as $(CO)_5Mn\text{-}Mn(CO)_3$(diimine), thus pointing towards homoleptic Os–Os bond breaking as a primary photoprocess. It was suggested that this reaction is most likely to occur from a reactive SBLCT state, populated as a result of surface crossing from an optically accessible MLCT state. Modification of the diimine ligand with redox-active groups, such as methyl viologen, allows for redox control of photoinduced charge-separation in this type of transition metal cluster [119].

Direct application of $Ru_3(CO)_{12}$ in photochemical synthesis has been described in detail [120]. Thermal reactions of this cluster in presence of two-electron donors L affords $[Ru_3(CO)_9L_3]$. The discovery in 1974 that irradiation of the cluster under those conditions produces mononuclear products instead of the substituted clusters initiated a wealth of research in Ru-clusters as precursors in photochemical synthesis [121]. Much research has been devoted to the preparation of mononuclear $\eta^2$-olefin complexes, as well as alkyne complexes. For example, $[Ru(CO)_3(PPh_3)_2]$ has been reported as an active catalyst for olefin polymerisation, and as such, many investigations have dealt with the reactivity of this compound. Other directions of research include formation of metallacycles, generation of new cluster species, and mixed transition metal/non-metal clusters.

## 3.7 Conclusions: What's Next for the Photochemistry of Metal Complexes?

Molecular inorganic photochemistry is extremely diverse. It lies at the very heart of many modern challenges—from fundamental understanding of reaction pathways with ever faster excitation sources, to applications in artificial photosynthesis and water splitting, radioisotopes separation, photocatalysis and photoelectrocatalysis. It involves all types of reaction occurring starting from the lowest, ground state, yet with the key difference that the reactions can only be initiated by light, and occur from much more energetic states.

It has long been acknowledged that the initial absorption of light creates a vibrationally hot, non-equilibrated excited state. However, only in the past decades has it become possible to follow the ultrafast events of vibrational energy dissipation and formation of thermally equilibrated excited states in real time. Thus the long expressed visionary ideas that photochemistry can be classified into 'ultrafast'—occurring from a non-equilibrated state—and 'slow', occurring form a thermally-equilibrated but electronically excited state—has finally gained experimental support.

Perhaps the most exciting feature of inorganic photochemistry is the presence of a much greater diversity of electronic excited states available within the range of usual excitation sources than is the case for organic compounds. Since many of these excited states are of different origin, and do not necessarily relax rapidly to the lowest excited state, the opportunities arise to control the products by changing the wavelength and the energy per pulse of the excitation light in a way that is not possible for pure organic compounds. Extension of these principles towards multimetallic species with unusual bonding provides another means to access reactive intermediates and photochemical products.

Selective excitation of transitions of different types leads to formation of different products—switching between dissociation, substitution or isomerisation, or purely photophysical processes when no new products are formed. Moreover, coordination of organic chromophores as ligands to metal centres allows ligand-centred transformations—such as isomerisation—to be performed under visible instead of UV light.

The 'modular' structure of metal-containing compounds, for example, $Ligand_1$-M-$Ligand_2$, offer an opportunity to alter the periphery of the metal complex so that it can be tuned for a specific application—such as anchoring to semiconductor surfaces in heterogeneous catalysis or dye-sensitised solar cells (see Chap. 7), or coupling to biological entities (see Chaps. 4, 9 and 10)—without altering significantly the orbital makeup and energy levels of the component parts, and hence the reaction pathways.

Bringing together the great diversity of excited states, the ultrafast means of initiating the transformations, the extremely sensitive modern means of detecting reactive intermediates, and novel theoretical methods to gain further insights into

electronic structure, dynamics and reactivity—the field of inorganic photochemistry will continue to make exciting contributions to fundamental and applied science.

## References


1. Turro NJ, Ramamurthy V, Scaiano JC (2009) Principles of molecular photochemistry. University Science Books, California, p 495
2. Roundhill DM (1994) Photochemistry and photophysics of metal complexes. Plenum Press, New York
3. Balzani V, Venturi M, Credi A (2008) Molecular devices and machines, 2nd edn. Wiley-VCH, Weinheim
4. Solomon EI, Lever ABP (eds) (2006) Inorganic electronic structure and spectroscopy, 2nd edn. Wiley, New York
5. Horvath O, Stevenson KL (1993) Charge transfer photochemistry of coordination compounds. Wiley-VCH, New York, p 380
6. Vlcek A (2000) The life and times of excited states of organometallic and coordination compounds. Coord Chem Rev 200–202:933–977
7. Vos JG, Pryce MT (2010) Photoinduced rearrangements in transition metal compounds. Coord Chem Rev 254:2519–2532
8. Muro ML, Rachford AA, Wang X, Castellano FN (2009) Photophysics of platinum(II) acetylides. In: Lees A (ed) Photophysics of organometallics, series: topics in organometallic chemistry, vol 29, pp 159–191
9. Butler JM, George MW, Schoonover JR et al (2007) Application of transient infrared and near infrared spectroscopy to transition metal complex excited states and intermediates. Coord Chem Rev 251:492–514
10. Adamson AW, Fleischauer PD (eds) (1975) Concepts of inorganic photochemistry. John Wiley & Sons, New York
11. Elsaesser T, Kaiser W (1991) Vibrational and vibronic relaxation of large polyatomic molecules in liquids. Annu Rev Phys Chem 42:83–107
12. Hochstrasser RM (2007) Multidimensional ultrafast spectroscopy. Proc Nat Acad Sci 104:14190–14196
13. Hunt NT (2009) 2D-IR spectroscopy: ultrafast insights into biomolecule structure and function. Chem Soc Rev 38:1837–1848
14. Schoonover JR, Strouse GF (1998) Time-resolved vibrational spectroscopy of electronically excited inorganic complexes in solution. Chem Rev 98:1335–1355
15. Best J, Sazanovich IV, Adams H et al (2010) Structure and ultrafast dynamics of the charge-transfer excited state and redox activity of the ground state of mono- and binuclear platinum(II) diimine catecholate and bis-catecholate complexes: A transient absorption, TRIR, DFT, and electrochemical study. Inorg Chem 49:10041–10056
16. Browne WR, McGarvey JJ (2007) The Raman effect and its application to electronic spectroscopies in metal-centered species: techniques and investigations in ground and excited states. Coord Chem Rev 251:454–473
17. Dyer RB, Woodruff WH (2007) Vibrational spectroscopy. In: Scott RA, Lukehart CM (eds) Applications of physical methods to inorganic and bioinorganic chemistry. John Wiley & Sons, Chichester
18. Coppens P (2011) Molecular excited-state structure by time-resolved pump probe X-ray diffraction. What is new and what are the prospects for further progress? J Phys Chem Lett 2:616–621

19. Coppens P, Gerlits O, Vorontsov II et al (2004) A very large Rh–Rh bond shortening on excitation of the $[Rh_2(1,8\text{-diisocyano-p-menthane})_4]^{2+}$ ion by time-resolved synchrotron X-ray diffraction. Chem Comm 2144–2145
20. Bressler C, Chergui M (2004) Ultrafast X-ray absorption spectroscopy. Chem Rev 104:1781–1812
21. Chergui M, Zewail AH (2009) Electron and X-Ray methods of ultrafast structural dynamics: advances and applications. Chem Phys Chem 10:28–43
22. Chen LX, Zhang X, Lockard JV et al (2010) Excited-state molecular structures captured by X-ray transient absorption spectroscopy: a decade and beyond. Acta Cryst A 66:240–251
23. Darr JA, Poliakoff M (1999) New directions in inorganic and metal-organic coordination chemistry in supercritical fluids. Chem Rev 99:495–541
24. Begel S, Heinemann FW, van Eldik R (2011) The classic "brown-ring" reaction in a new medium: Kinetics, mechanism, and spectroscopy of the reversible binding of nitric oxide to iron(II) in an ionic liquid. Inorg Chem 50:3946–3958
25. Cotton AF, Wilkinson G (1972) Advanced inorganic chemistry, 3rd edn. Wiley, New York, pp 555–620
26. Ford PC (1982) The ligand-field photosubstitution reactions of $d^6$ hexacoordinate metal complexes. Coord Chem Rev 44:61–82
27. Weinstein JA, Grills DC, Towrie M et al (2002) Picosecond time-resolved infrared spectroscopic investigation of excited state dynamics in a Pt(II) diimine chromophore. Chem Comm 382–383
28. Yam VWW, Wong KM, Zhu N (2002) Solvent-induced aggregation through metal center dot center dot center dot metal/pi center dot center dot center dot pi interactions: large solvatochromism of luminescent organoplatinum(II) terpyridyl complexes. J Am Chem Soc 124:6506–6507
29. Chan CW, Cheng LK, Che CM (1994) Luminescent donor-acceptor platinum(II) complexes. Coord Chem Rev 132:87–97
30. Hissler M, Connick WB, Geiger DK et al (2000) Platinum diiminebis (acetylide) complexes: synthesis, characterization, and luminescence properties. Inorg Chem 39:447–457
31. Keller JM, Glusac KD, Danilov EO et al (2011) Negative polaron and triplet exciton diffusion in organometallic "molecular wires". J Am Chem Soc 133:11289–11298
32. Lu W, Mi B-X, Chan MCW et al (2004) Light-emitting tridentate cyclometalated platinum(II) complexes containing sigma-alkynyl auxiliaries: Tuning of photo- and electrophosphorescence. J Am Chem Soc 126:4958–4971
33. Lu W, Chan MCW, Cheung KK et al (2001) Interactions in organometallic systems. Crystal structures and spectroscopic properties of luminescent mono-, bi-, and trinuclear trans-cyclometalated platinum(II) complexes derived from 2,6 diphenylpyridine. Organometallics 20:2477–2486
34. Williams JAG, Beeby A, Davies ES et al (2003) An alternative route to highly luminescent platinum(II) complexes: cyclometalation with N^C^N-coordinating dipyridylbenzene ligands. Inorg Chem 42:8609–8611
35. Michalec JF, Bejune SA, McMillin DR (2000) Multiple ligand-based emissions from a platinum(II) terpyridine complex attached to pyrene. Inorg Chem 39:2708–2709
36. Sazanovich IV, Alamiry MAH, Best J et al (2008) Excited state dynamics of a Pt(II) diimine complex bearing a naphthalene-diimide electron acceptor. Inorg Chem 47:10432–10445
37. Yarnell JE, Deaton JC, McCusker CE et al (2011) Bidirectional "ping-pong" energy transfer and 3000-fold lifetime enhancement in a Re(I) charge transfer complex. Inorg Chem 50:7820–7830
38. Yeh AT, Shank CV, McCusker JK (2000) Ultrafast electron localization dynamics following photo-induced charge transfer. Science 289:935–938
39. Cannizzo A, van Mourik F, Gawelda W et al (2006) Broadband femtosecond fluorescence spectroscopy of $[Ru(bpy)_3]^{2+}$. Angew Chem Int Ed 45:3174–3176

40. Van Houten J, Watts RJ (1976) Temperature dependence of photophysical and photochemical properties of tris(2,2′-bipyridyl))ruthenium ion in aqueous solution. J Am Chem Soc 98:4853–4858
41. Lehn JM, Ziessel R (1982) Photochemical generation of carbon-monoxide and hydrogen by reduction of carbon dioxide and water under visible light irradiation. Proc Natl Acad Sci USA 79:701–704
42. Burrows HD, Kemp TJ (1974) Photochemistry of uranyl-ion. Chem Soc Rev 3:139–165
43. Redmond MP, Cornet SM, Woodall SD et al (2011) Probing the local coordination environment and nuclearity of uranyl(VI) complexes in non-aqueous media by emission spectroscopy. Dalton Trans 40:3914–3926
44. Schwarz G (2005) Molybdenum cofactor biosynthesis and deficiency. Cell Mol Life Sci 62:2792–2810
45. Hsu JK, Bonangelino CJ, Kaiwar SP et al (1996) Direct conversion of alphasubstituted ketones to metallo-1,2-enedithiolates. Inorg Chem 35:4743–4751
46. Bevilacqua JM, Eisenberg R (1994) Synthesis and characterization of luminescent square-planar platinum(II) complexes containing dithiolate or dithiocarbamate ligands. Inorg Chem 33:2913–2923
47. Weinstein JA, Zheligovskaya NN, Mel'nikov MY et al (1998) Spectroscopic (UV/VIS, resonance Raman) and spectroelectrochemical study of platinum(II) complexes with 2,2 '-bipyridine and aromatic thiolate ligands. J Chem Soc Dalton Trans 2459–2466
48. McInnes, EJL, Farley RD, Rowlands CC et al (1999) On the electronic structure of [Pt(4,4′-$X_2$-bipy)$Cl_2$](0/-/2-): an electrochemical and spectroscopic (UV/Vis, EPR, ENDOR) study. J Chem Soc Dalton Trans 4203–4208
49. Shavaleev NM, Davies ES, Adams H et al (2008) Platinum(II) diimine complexes with catecholate ligands bearing imide electron-acceptor groups: Synthesis, crystal structures (spectro) electrochemical and EPR studies, and electronic structure. Inorg Chem 47:1532–1547
50. Galin AM, Razskazovsky YV, Melnikov MY (1994) The photochemistry of mixed-ligand complexes $(ArS)_2$ZnPhen with the lowest ligand–ligand charge transfer excited state. J Photochem Photobiol A: Chem 78:113–117
51. Whittle CE, Weinstein JA, George MW, Schanze KS (2001) Photophysics of diimine platinum (II) bis-acetylide complexes. Inorg Chem 40:4053–4062
52. Aarnts MP, Wilms MP, Peelen K et al (1996) Bonding properties of a novel inorganometallic complex, Ru(SnPh3)2(CO)2(iPr-DAB) (iPr-DAB = N, N′-diisopropyl-1,4-diaza-1,3-butadiene), and its stable radical-anion, studied by UVVis, IR, and EPR spectroscopy (spectro-)electrochemistry, and density functional calculations. Inorg Chem 35:5468–5477
53. van Slageren J, Hartl F, Stufkens DJ et al (2000) Changes in excited-state character of [M(L-1)(L-2)$(CO)_2$(alpha-diimine)] (M = Ru, Os) induced by variation of L-1 and L-2. Coord Chem Rev 208:309–320
54. Rossenaar BD, Stufkens DJ, Vlcek A Jr (1996) Halide-dependent change of the lowest-excited-state character from MLCT to XLCT for the complexes Re(X)$(CO)_3$(alpha-diimine) (X = Cl, Br, I; alpha-diimine equals bpy, iPr-PyCa, iPr-DAB) studied by resonance Raman, time-resolved absorption, and emission spectroscopy. Inorg Chem 35:2902–2909
55. Niewenhuis HA, Stufkens DJ, Oskam A (1994) Remarkable influence of X and R on the charge-transfer character (MLCT or XLCT) of the complexes [Ru(X)(R)$(CO)_2$(L)] (X = halide, $CF_3SO_3$ R = alkyl L = alpha-diimine)–a UV-VIS absorption and resonance Raman study. Inorg Chem 33:3212–3217
56. Pettijohn CN, Jochnowitz EB, Chuong B et al (1998) Luminescent excimers and exciplexes of Pt-II compounds. Coord Chem Rev 171:85–92
57. Roundhill DM, Gray HB, Che CM (1989) Pyrophosphito-bridged diplatinum chemistry. Acc Chem Res 22:55–61
58. Kim CD, Pillet S, Wu G et al (2002) Excited-state structure by time-resolved X-ray diffraction. Acta Cryst A 58(2):133–137

59. van der Veen RM, Milne C, El Nahhas A et al (2009) Structural determination of a photochemically active diplatinum molecule by time-resolved EXAFS spectroscopy. Angew Chem Int Ed 48:2711–2714
60. Novozhilova IV, Volkov AV, Coppens P (2003) Theoretical analysis of the triplet excited state of the $[Pt_2(H_2P_2O_5)_4]^{4-}$ ion and comparison with time resolved X-ray and spectroscopic results. J Am Chem Soc 125:1079–1087
61. Cotton FA, Murillo C, Walton RA (2005) Multiple bonds between metal atoms, 3rd edn. Springer Science, New York
62. Cotton FA, Nocera DG (2000) The whole story of the two-electron bond, with the delta bond as a paradigm. Acc Chem Res 33:483–490
63. Hopkins MD, Gray HB (1984) Nature of the emissive excited state of quadruply bonded $Mo_2X_4(PMe_3)_4$ complexes. J Am Chem Soc 106:2468–2469
64. Chang IJ, Nocera DG (1989) Oxidation photochemistry of dimolybdenum(II) diaryl phosphate promoted by visible-light. Inorg Chem 28:4311–4312
65. Caspar JV, Kober EM, Sullivan BP et al (1982) Application of the energy gap law to the decay of charge-transfer excited states. J Am Chem Soc 104:630–632
66. Alberding BG, Chisholm MH, Gustafson TL (2012) Detection of the singlet and triplet MM delta delta* states in quadruply bonded dimetal tetracarboxylates (M = Mo, W) by time-resolved infrared spectroscopy. Inorg Chem 51:491–498
67. Alberding BG, Chisholm MH, Gallucci JC et al (2011) Electron delocalization in the S-1 and T-1 metal-to-ligand charge transfer states of transsubstituted metal quadruply bonded complexes. Proc Natl Acad Sci USA 108:8152–8156
68. Chisholm MH (2012) Incorporating MM quadruple bonds into conjugated organic oligomers: syntheses and optoelectronic properties. Macromol Chem Phys 213:800–807
69. McQuillin FJ, Parker DG, Stephenson GR (1991) Transition metal organometallics for organic synthesis. Cambridge University Press, Cambridge
70. Geoffroy GL, Wrighton MS (1979) Organometallic photochemistry. Academic Press, New York
71. Turner JJ, Burdett JK, Perutz RN et al (1977) Matrix photochemistry of metal-carbonyls. Pure Appl Chem 49:271–285
72. Bonneau R, Kelly JM (1980) Flash photolysis of chromium hexacarbonyl in perfluorocarbon solvents—observation of a highly reactive chromium pentacarbonyl. J Am Chem Soc 102:1220–1221
73. Mond L, Langer C, Quincke F (1890) Action of carbon monoxide on nickel. J Chem Soc Trans 57:749–753
74. Long C (2010) Photophysics of CO loss from simple metal carbonyl complexes. In: Lees AJ (ed) Photophysics of organometallics. Topics in organometallic chemistry, vol 29, pp 37–71
75. Poliakoff M, Turner JJ (2001) The structure of $[Fe(CO)_4]$—an important new chapter in a long-running story. Angew Chem Int Ed 40:2809–2812
76. Portius P, Yang J, Grills DC et al (2004) Unraveling the photochemistry of $Fe(CO)_5$ in solution. J Am Chem Soc 126:10713–10720
77. Lian T, Bromberg SE, Asplund MC et al (1996) Femtosecond infrared studies of the dissociation and dynamics of transition metal carbonyls in solution. J Phys Chem 100:11994–12001
78. Nasielski J, Colas A (1978) Primary process in photochemistry of group 6B metal hexacarbonyls 2. Inorg Chem 17:237–240
79. Dahlgren RM, Zink JI (1977) Ligand substitution photochemistry of monosubstituted derivatives of tungsten hexacarbonyl. Inorg Chem 16:3154–3161
80. Cooper AI, Poliakoff M (1993) High pressure reactions in polyethylene films. Chem Phys Lett 212:611–616
81. Kobayashi T, Yasufuku K, Iwai J et al (1985) Laser photolysis study of the photosubstitution in dimanganese and dirhenium decacarbonyls. Coord Chem Rev 64:1–19

82. Firth S, Hodges PM, Poliakoff M et al (1987) Selective loss of CO in the photochemistry of $MnRe(CO)_{10}$—a study using matrix isolation and time-resolved infrared spectroscopy. J Organomet Chem 331:347–355
83. Rimmer RD, Richter H, Ford PC (2010) A photochemical precursor for carbon monoxide release in aerated aqueous media. Inorg Chem 49:1180–1185
84. Kunkely H, Vogler A (2004) Ligand-to-ligand charge transfer in Mo(diphos)(CO)(NO)(dtc) with diphos = 1,2-bis(diphenylphosphino)ethane and dtc(-) = dimethyldithiocarbamate. Spectroscopy and photochemistry. Inorg Chem Commun 7:767–769
85. Dattelbaum DM, Itokazu MK, Iha NYM et al (2003) Mechanism of metal-to-ligand charge transfer sensitization of olefin trans-to-cis isomerization in the fac-$[Re^{I}(phen)(CO)_3(1,2\text{-}bpe)]^+$ cation. J Phys Chem A 107:4092–4095
86. Coleman A, Draper SM, Long C et al (2007) Photochemical cis-trans isomerization of cis-(eta(6)-1,2-diphenylethene)$Cr(CO)_3$ and the molecular structure of trans-(eta(6)-1,2-diphenylethene)$Cr(CO)_3$. Organometallics 26:4128–4134
87. Busby M, Hartl F, Matousek P et al (2008) Ultrafast excited state dynamics controlling photochemical isomerization of N-methyl-4-[trans-2-(4-pyridyl)ethenyl]pyridinium coordinated to a Re(CO)3(2,2′-bipyridine) chromophore. Chem Eur J 14:6912–6923
88. Patrocinio AOT, Iha NYM (2008) Photoswitches and luminescent rigidity sensors based on fac-$[Re(CO)_3(Me_4phen)(L)]^+$. Inorg Chem 47:10851–10857
89. Bitterwolf TE (2006) Photochemical nitrosyl linkage isomerism/metastable states. Coord Chem Rev 250:1196–1207
90. Rack JJ (2009) Electron transfer triggered sulfoxide isomerization in ruthenium and osmium complexes. Coord Chem Rev 253:78–85
91. Srajer V, Teng TY, Ursby T et al (1996) Photolysis of the carbon monoxide complex of myoglobin: nanosecond time-resolved crystallography. Science 274:1726–1729
92. Carducci MD, Pressprich MR, Coppens P (1997) Diffraction studies of photoexcited crystals: metastable nitrosyl-linkage isomers of sodium nitroprusside. J Am Chem Soc 119:2669–2678
93. Manoharan PT, Gray HB (1966) Electronic structure of metal pentacyanonitrosyls. Inorg Chem 5:823–839
94. Schaniel D, Woike T (2009) Necessary conditions for the photogeneration of nitrosyl linkage isomers. Phys Chem Chem Phys 11:4391–4395
95. Warren MR, Brayshaw SK, Johnson AL et al (2009) Reversible 100% linkage isomerization in a single-crystal to single-crystal transformation: photocrystallographic identification of the metastable [Ni(dppe)($\eta^1$-ONO)Cl] isomer. Angew Chem Int Ed 48:5711–5714
96. Hatcher LE, Warren MR, Allan DR et al (2011) Metastable linkage isomerism in $[Ni(Et_4dien)(NO_2)_2]$: a combined thermal and photocrystallographic structural investigation of a nitro/nitrito interconversion. Angew Chem Int Ed 50:8371–8374
97. Hesek D, Inoue Y, Ishida H et al (2000) The first asymmetric synthesis of chiral ruthenium tris(bipyridine) from racemic ruthenium bis(bipyridine) complexes. Tetrahedron Lett 41:2617–2620
98. Durham B, Wilson SR, Hodgson DJ et al (1980) Cis-trans photoisomerisation in $Ru(bpy)_2(OH_2)_2^{2+}$—crystal structure of trans-$[Ru(bpy)_2(OH_2)(OH)](ClO_4)_2$. J Am Chem Soc 102:600–607
99. Tamayo AB, Alleyne BD, Djurovich PI et al (2003) Synthesis and characterization of facial and meridional tris-cyclometalated iridium(III) complexes. J Am Chem Soc 125:7377–7387
100. Osman R, Perutz RN, Rooney AD et al (1994) Picosecond photolysis of a metal dihydride—rapid reductive elimination of dihydrogen from $Ru(DMPE)_2H_2$ (Dmpe = $(CH_3)_2PCH_2CH_2P(CH_3)_2$). J Phys Chem 98:3562–3563
101. Chatt J, Davidson JM (1965) The tautomerism of arene and ditertiary phosphine complexes of Ruthenium(0), and the preparation of new types of hydrido-complexes of ruthenium(II). J Chem Soc 843–855
102. Hoyano JK, Graham WAG (1982) Hydrogen-mediated photolysis of ($\eta^5$-$C_5Me_5$)$Os(CO)_2H$. J Am Chem Soc 104:3723–3725

103. Janowicz AH, Bergman RC (1982) C–H activation in completely saturated hydrocarbons. J Am Chem Soc 104:352–354
104. Solari E, Da Silva C, Iacono B et al (2001) Photochemical activation of the NN bond in a dimolybdenum-dinitrogen complex: formation of a molybdenum nitride. Angew Chem Int Ed 40:3907–3909
105. Curley JJ, Cook TR, Reece SY et al (2008) Shining light on dinitrogen cleavage: structural features, redox chemistry, and photochemistry of the key intermediate bridging dinitrogen complex. J Am Chem Soc 130:9394–9405
106. Kunkely H, Vogler A (2010) Photolysis of aqueous $[(NH_3)_5Os(N_2)Os(NH_3)_5]^{5+}$: cleavage of dinitrogen by an intramolecular photoredox reaction. Angew Chem Int Ed 49:1591–1593
107. Archer S, Weinstein JA (2012) Coord Chem Rev Charge-separated excited states in Platinum(II) chromophores: photophysics, formation, stabilization and utilization in solar energy conversion. Coord Chem Rev 256:2530–2561
108. Johnson BFG (1980) In: Johnson BFG (ed) Transition metal clusters. Wiley, UK
109. Braunstein P, Oro LA, Raithby PR (eds) (1999) Metal clusters in chemistry. Wiley-VCH, Weinheim
110. Vergeer FW, Hartl F, Matousek P et al (2002) First direct observation of a CO-bridged primary photoproduct of $[Ru_3(CO)_{12}]$ by picosecond time-resolved IR spectroscopy. Chem Commun 1220–1221
111. Ford PC (1990) Quantitative mechanistic studies of the photoreactions of trinuclear metal-carbonyl clusters of iron, ruthenium and osmium. J Organomet Chem 383:339–356
112. DiBenedetto JA, Ryba DW, Ford PC (1989) Reaction dynamics of photosubstitution intermediates of the tri-ruthenium cluster $Ru_3(CO)_{12}$ as studied by flash photolysis with infrared detection. Inorg Chem 28:3503–3507
113. Bentsen JG, Wrighton MS (1987) Wavelength-dependent primary photoprocesses of $Os_3(CO)_{12}$ in fluid solution and in rigid alkane glasses at low temperature: spectroscopic detection, characterization, and reactivity of coordinatively unsaturated $Os_3(CO)_{11}$. J Am Chem Soc 109:4518–4530
114. Roberts DA, Geoffroy GL (1982) In comprehensive organometallic chemistry, vol 6. Pergamon, Oxford
115. Farrugia LJ (1995) In comprehensive organometallic chemistry II, vol 10. Pergamon, New York
116. Hunstock E, Mealli C, Calhorda MJ et al (1999) Molecular structures of $M_2(CO)_9$ and $M_3(CO)_{12}$ (M = Fe, Ru, Os): new theoretical insights. Inorg Chem 38:5053–5060
117. Nijhoff J, Hartl F, Stufkens DJ et al (1999) Light-induced insertion of a CO ligand into an Os-N bond of the clusters $Os_3(CO)_{10}(L)$, where L represents a potentially terdentate N, N′-chelating alpha-diimine. Organometallics 18:4380–4389
118. Nijhoff J, Bakker MJ, Hartl F et al (1998) Photochemistry of the triangular clusters $Os_3(CO)_{10}$(alpha-diimine): Homolysis of an Os–Os bond and solvent dependent formation of biradicals and zwitterions. Inorg Chem 37:661–668
119. Vergeer FW, Kleverlaan CJ, Matousek P et al (2005) Redox control of light induced charge separation in a transition metal cluster: photochemistry of a methyl viologen-substituted $[Os_3(CO)_{10}$(alpha-diimine)] cluster. Inorg Chem 44:1319–1331
120. Leadbeater NE (1995) The generation and reactivity of versatile ruthenium carbonyl organometallic intermediates by cluster photochemistry. J Chem Soc Dalton Trans 2923–2934
121. Johnson BFG, Lewis J, Twigg MV (1974) Photochemical reactions of $Ru_3(CO)_{12}$ involving metal–metal bond fission. J Organomet Chem 67:C75–C76